

R. Ludwig and G. Bogdanov
“RF Circuit Design: Theory and Applications”
2nd edition

Figures for Chapter 5

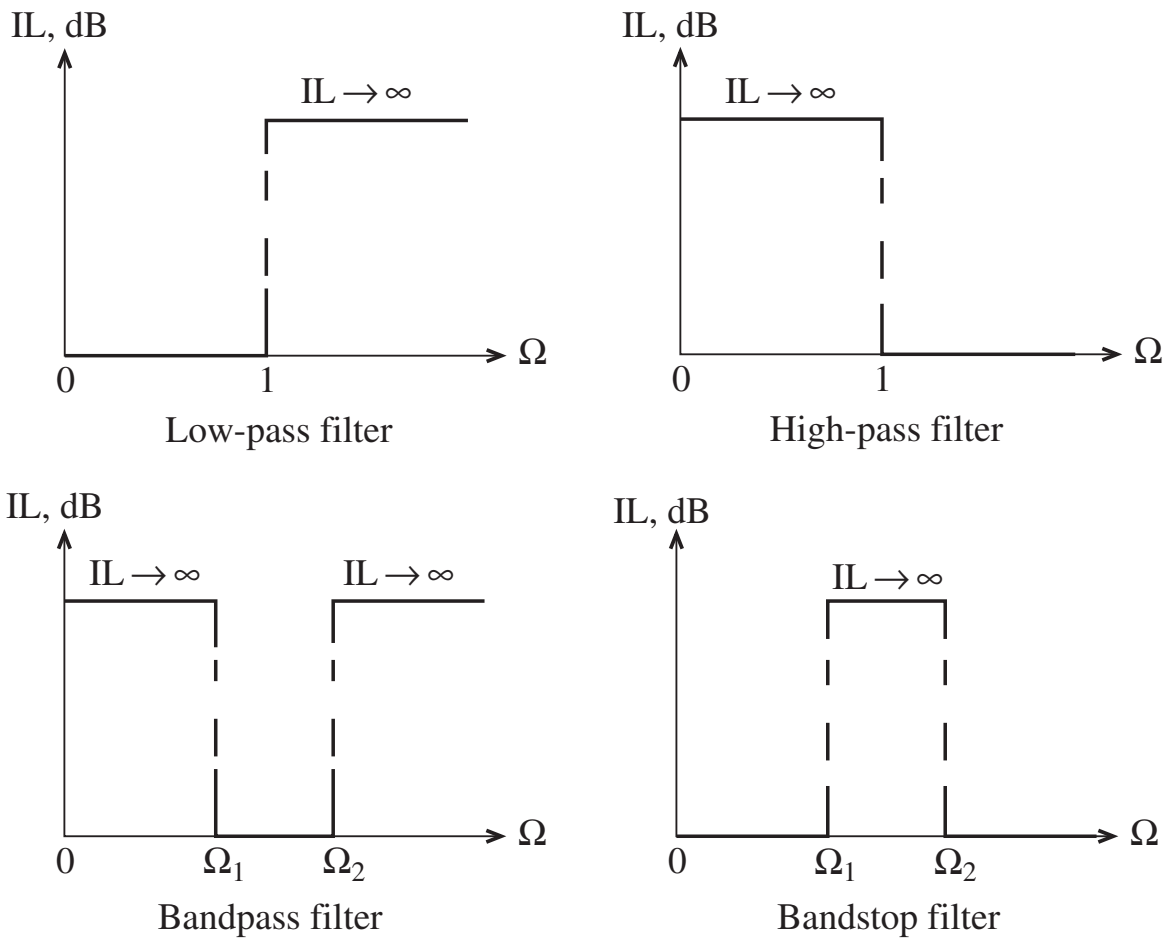


Figure 1-1 Four basic filter types.

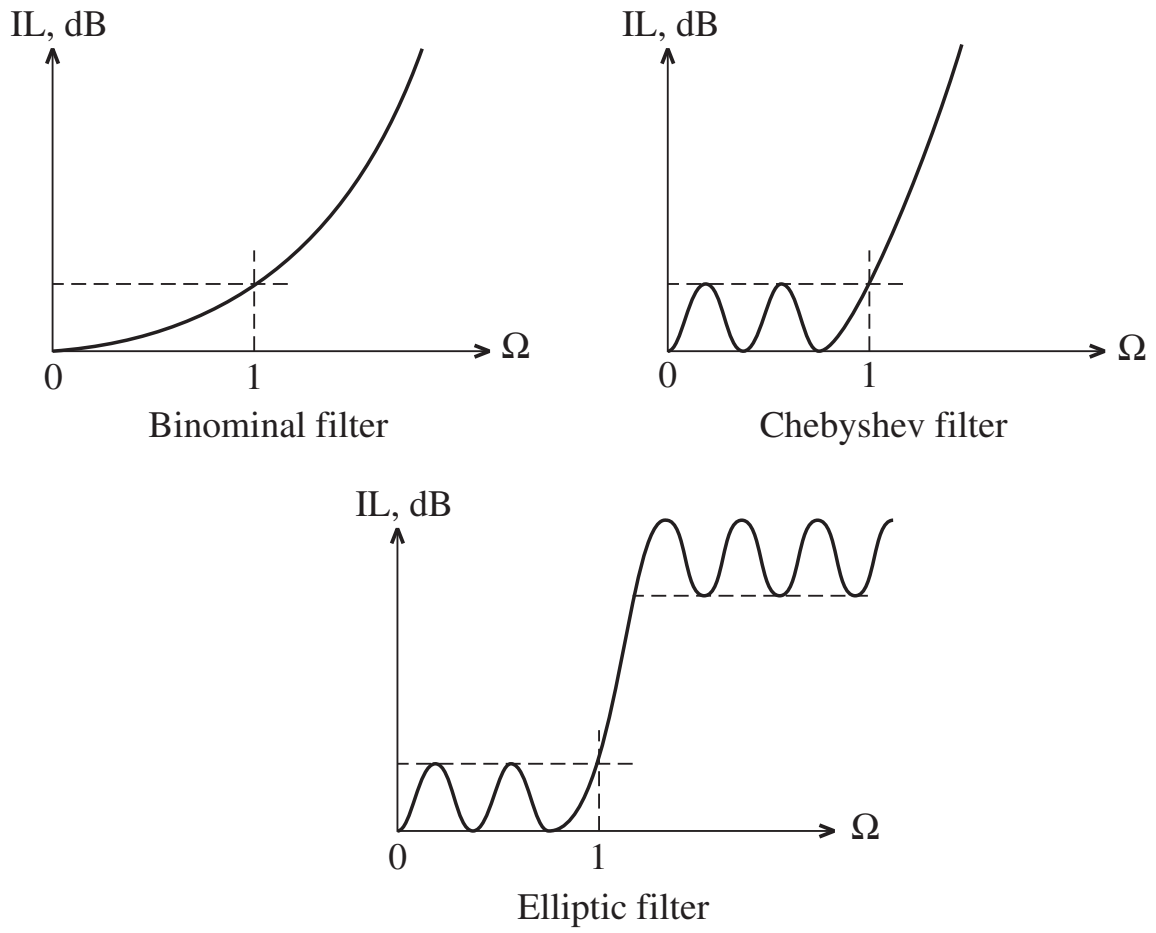


Figure 1-2 Actual attenuation profile for three types of low-pass filters.

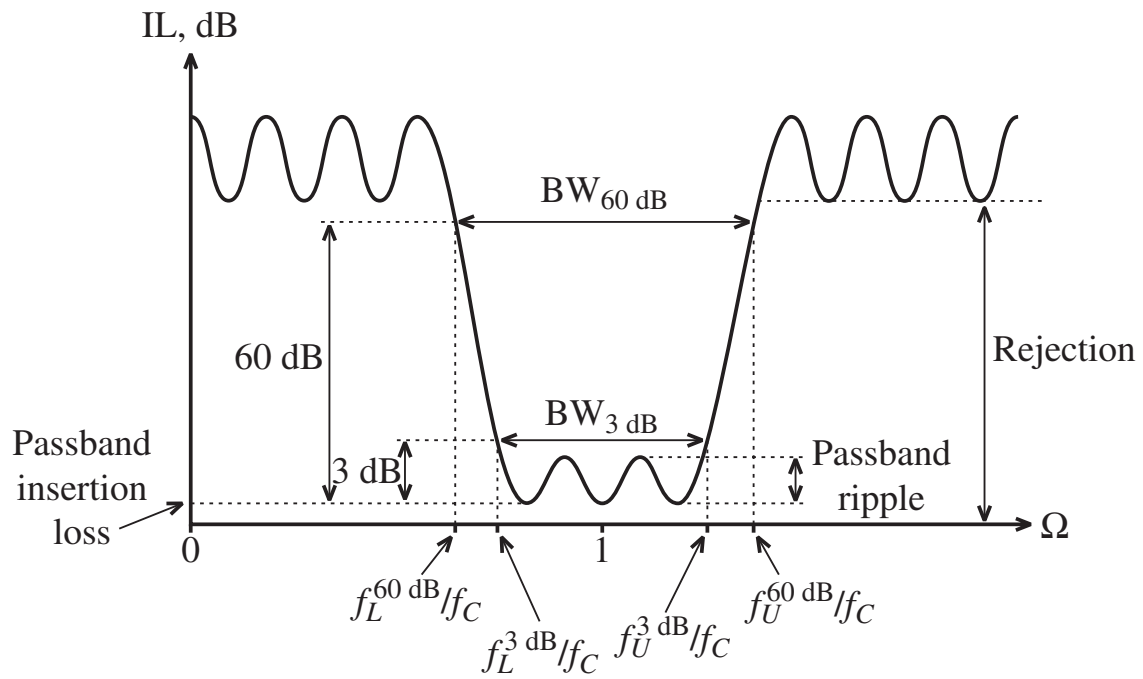


Figure 1-3 Generic attenuation profile for a bandpass filter.

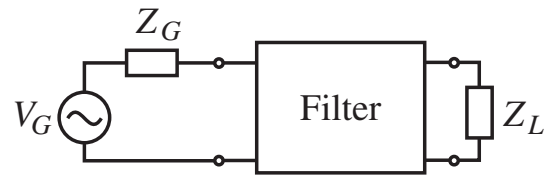


Figure 1-4 Filter as a two-port network connected to an RF source and load.

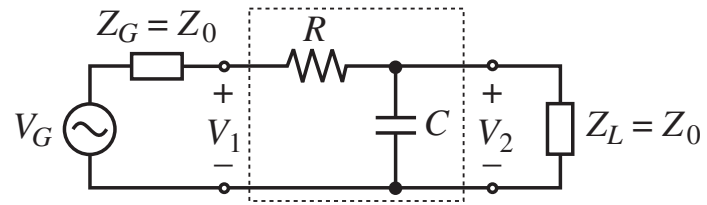


Figure 1-5 Low-pass filter connected between a source and load.

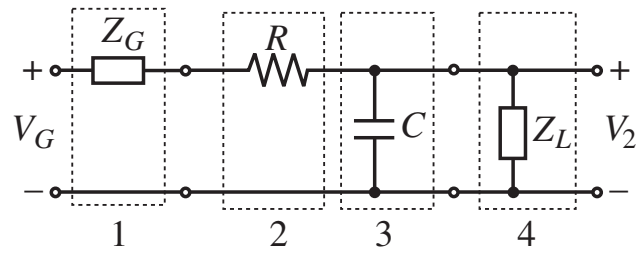
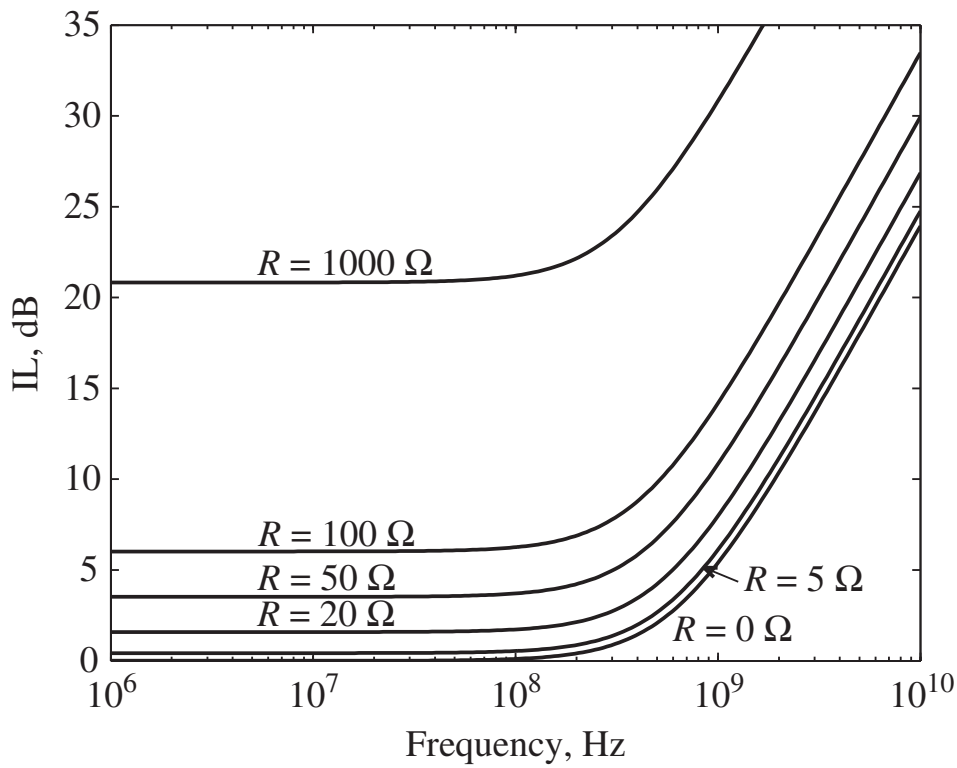
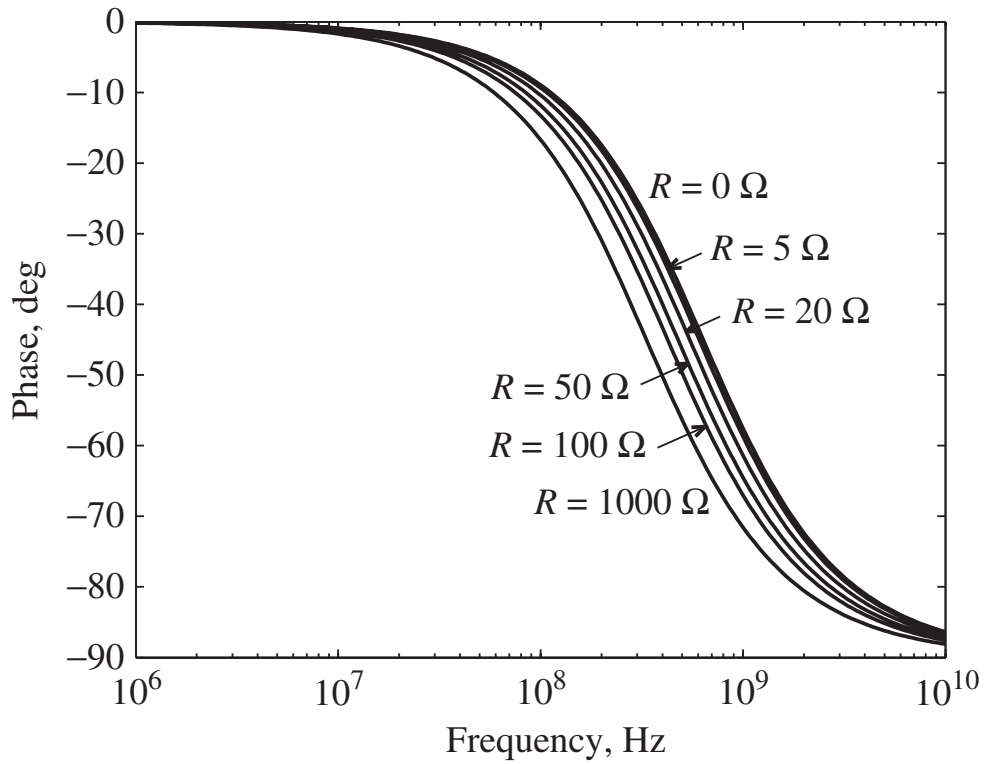


Figure 1-6 Cascading four *ABCD* networks.

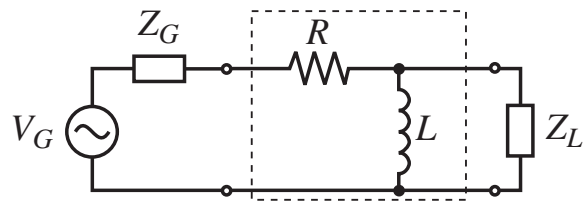


(a) Attenuation profile

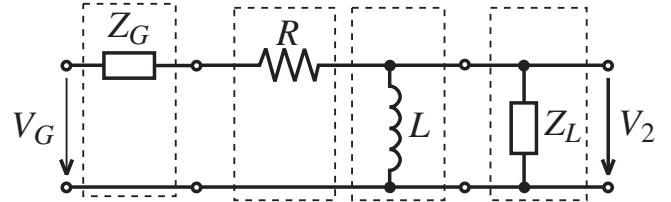


(b) Phase response

Figure 1-7 First-order low-pass filter response as a function of various parasitic resistance values.

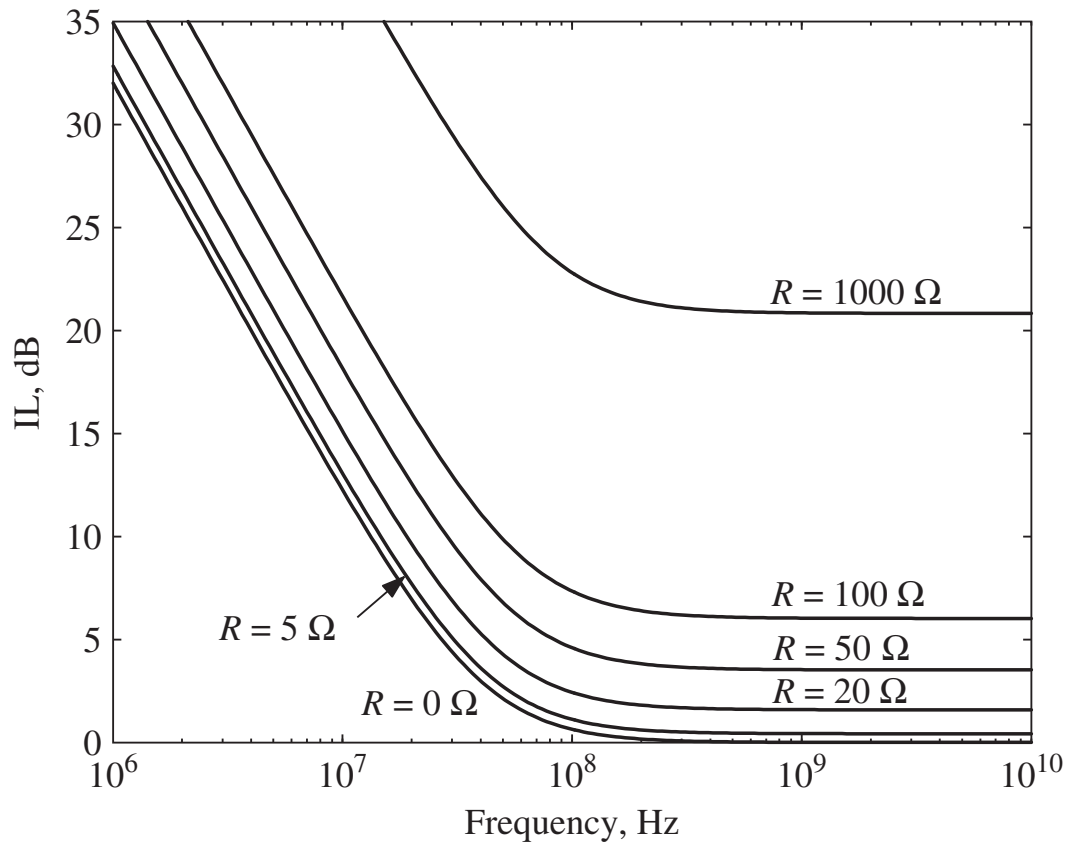


(a) High-pass filter with load resistance

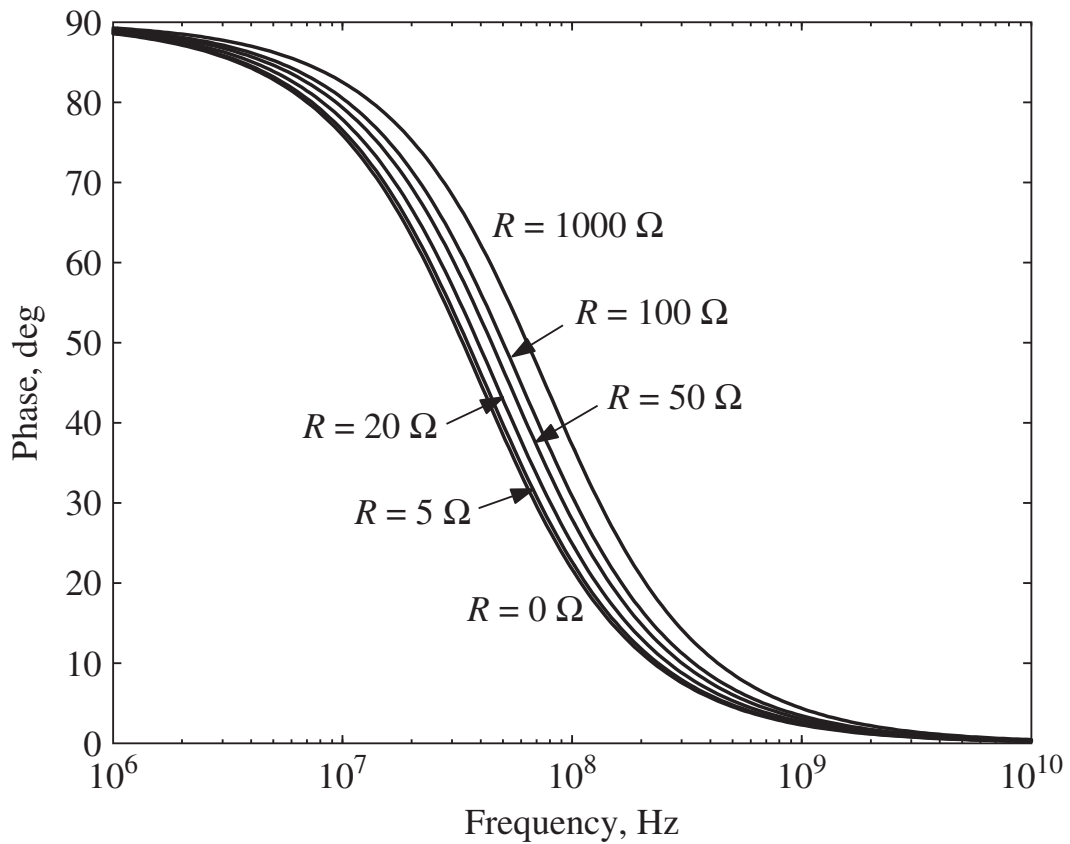


(b) Network and input/output voltages

Figure 1-8 First-order high-pass filter.



(a) Attenuation profile



(b) Phase response

Figure 1-9 High-pass filter response as a function of various parasitic resistance values.

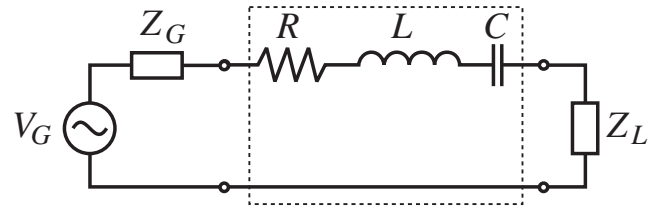


Figure 1-10 Bandpass filter implemented in series configuration.

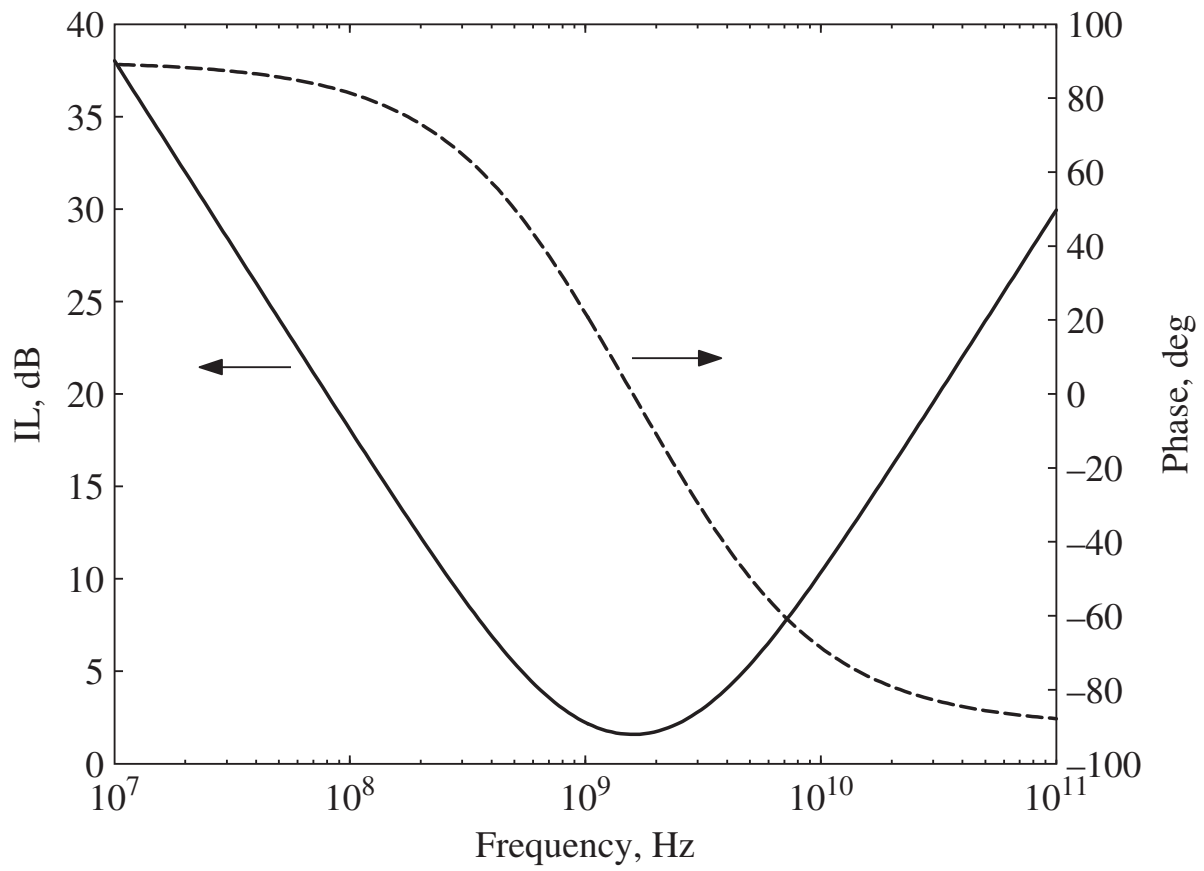
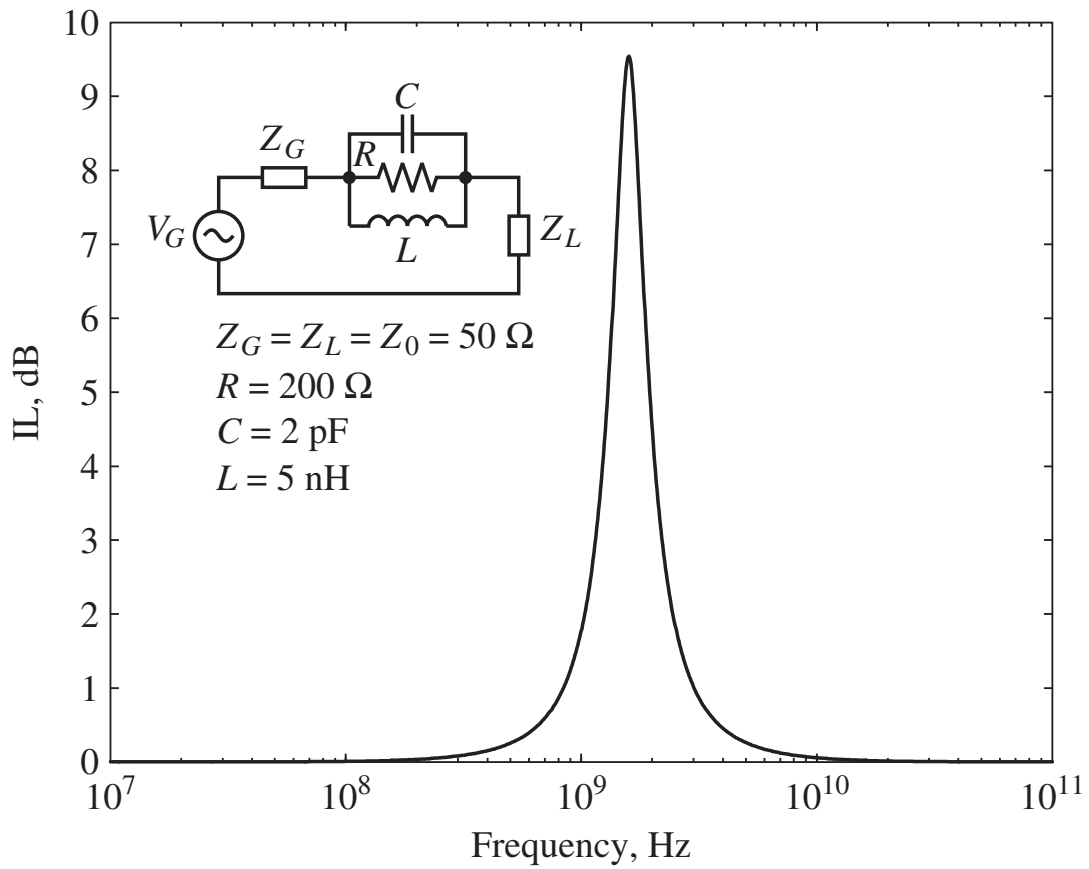
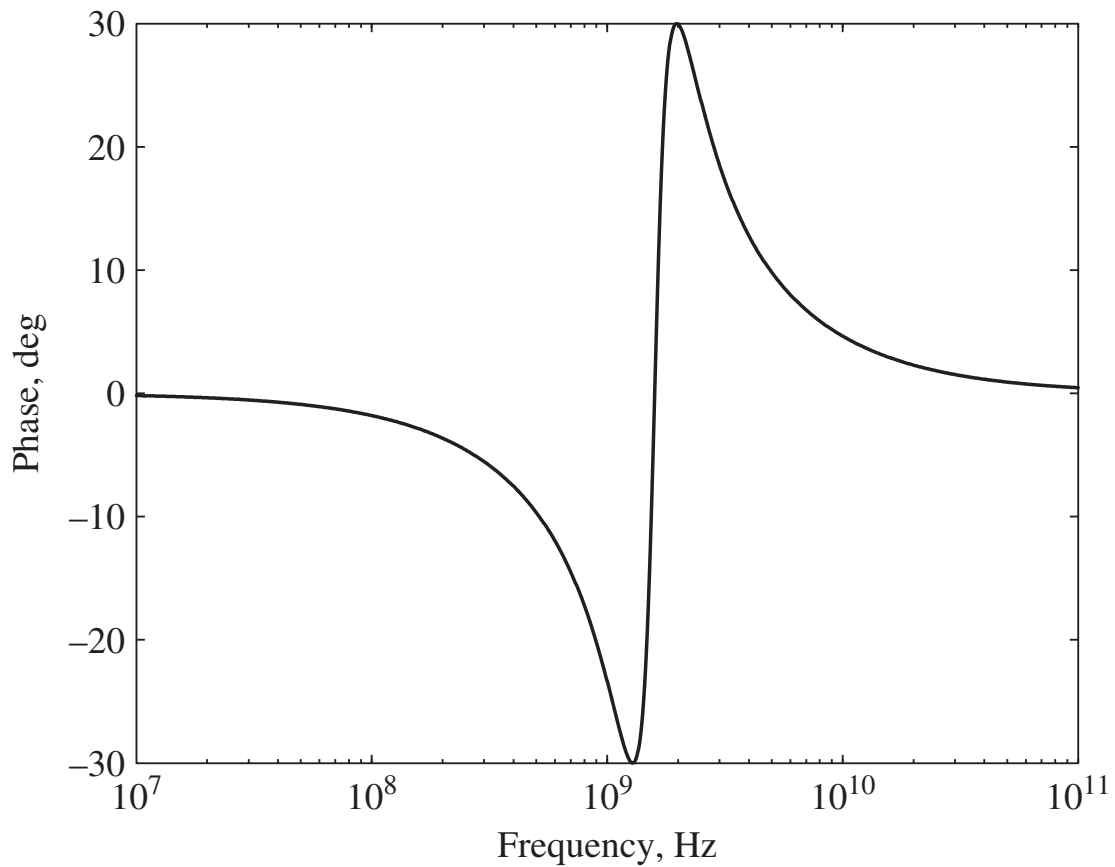


Figure 1-11 Bandpass filter response.




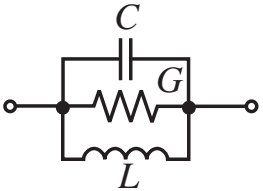
(a) Magnitude of transfer function



(b) Phase of transfer function

Figure 1-12 Bandstop filter response.

Table 1-1 Series and parallel resonators

<p>Parameter</p>		
<p>Impedance or Admittance</p>	$Z = R + j\omega L + \frac{1}{j\omega C}$	$Y = G + j\omega C + \frac{1}{j\omega L}$
<p>Resonance Frequency</p>	$\omega_0 = \frac{1}{\sqrt{LC}}$	$\omega_0 = \frac{1}{\sqrt{LC}}$
<p>Dissipation Factor</p>	$d = \frac{R}{\omega_0 L} = R\omega_0 C$	$d = \frac{G}{\omega_0 C} = G\omega_0 L$
<p>Quality Factor</p>	$Q = \frac{\omega_0 L}{R} = \frac{1}{R\omega_0 C}$	$Q = \frac{\omega_0 C}{G} = \frac{1}{G\omega_0 L}$
<p>Bandwidth</p>	$\text{BW} = \frac{f_0}{Q} = \frac{1}{2\pi L} \frac{R}{C}$	$\text{BW} = \frac{f_0}{Q} = \frac{1}{2\pi C} \frac{G}{L}$

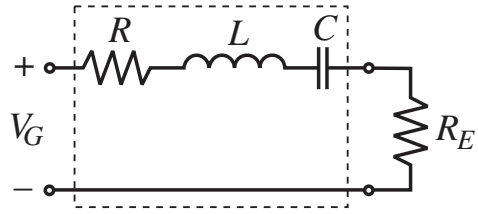
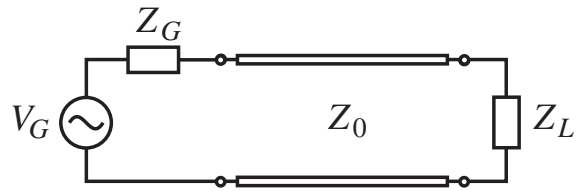
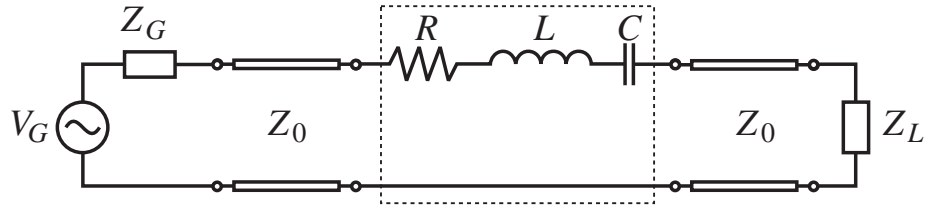


Figure 1-13 Circuit used for the definitions of loaded and unloaded quality factors.



(a) Matched transmission line system.



(b) Insert bandpass filter.

Figure 1-14 Insertion loss considerations.

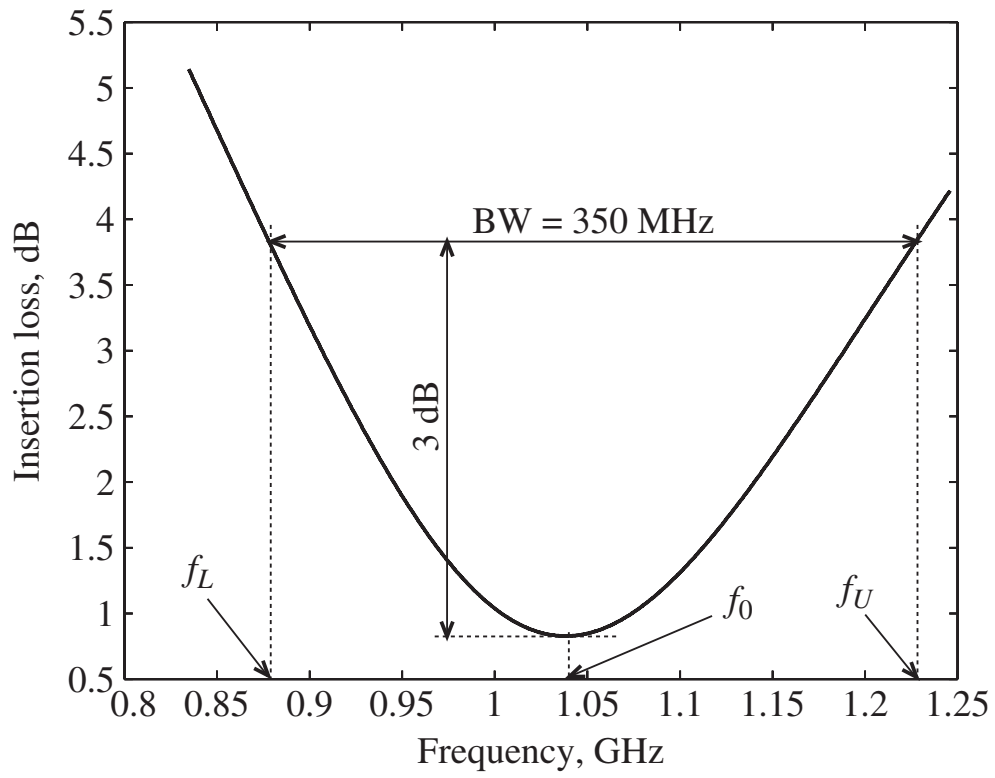


Figure 1-15 Insertion loss versus frequency.

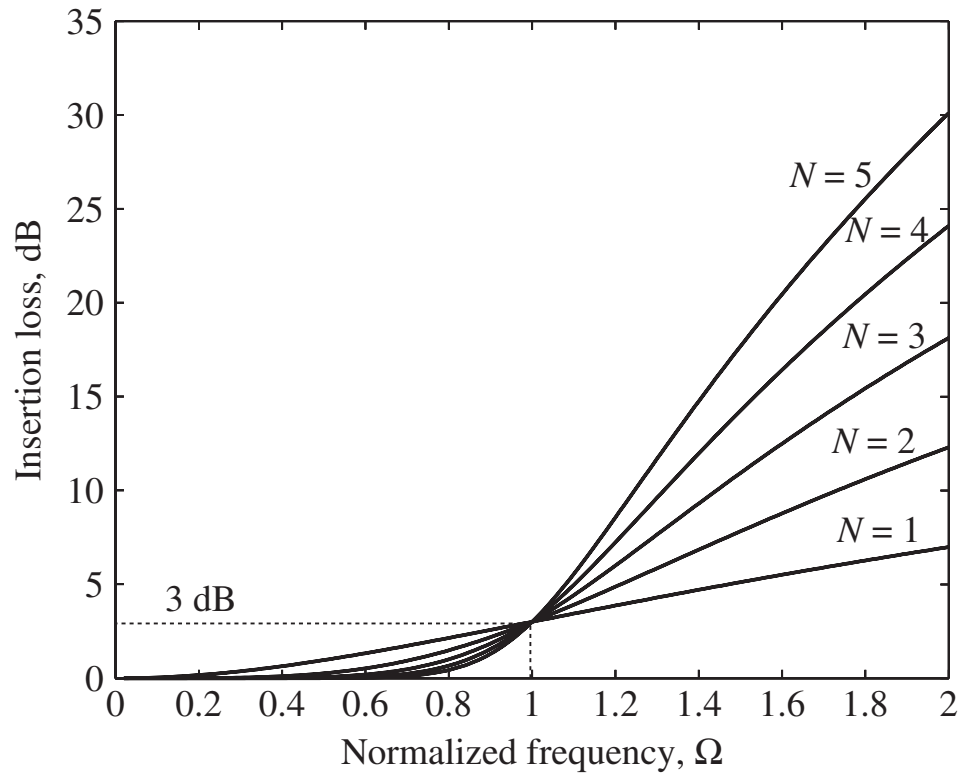
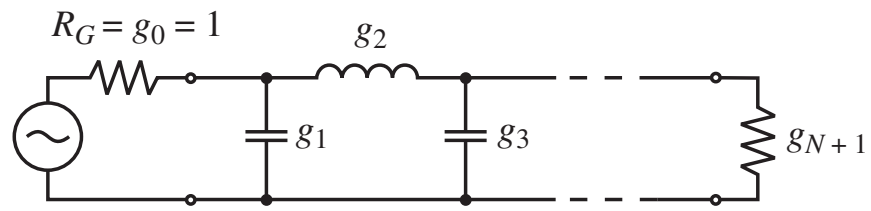
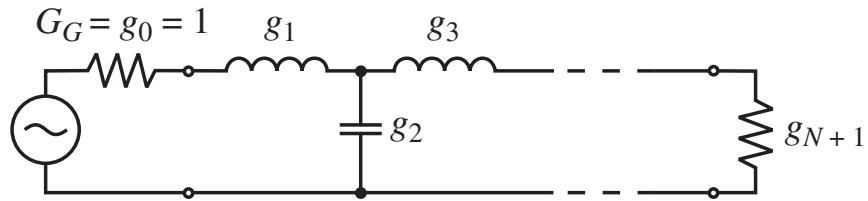


Figure 1-16 Butterworth low-pass filter design.



(a)



(b)

Figure 1-17 Two equivalent realizations of the generic multisection low-pass filter with normalized elements.

Table 1-2 Coefficients for maximally flat low-pass filter ($N = 1$ to 10)

N	g_1	g_2	g_3	g_4	g_5	g_6	g_7	g_8	g_9	g_{10}	g_{11}
1	2.0000	1.0000									
2	1.4142	1.4142	1.0000								
3	1.0000	2.0000	1.0000	1.0000							
4	0.7654	1.8478	1.8478	0.7654	1.0000						
5	0.6180	1.6180	2.0000	1.6180	0.6180	1.0000					
6	0.5176	1.4142	1.9318	1.9318	1.4142	0.5176	1.0000				
7	0.4450	1.2470	1.8019	2.0000	1.8019	1.2470	0.4450	1.0000			
8	0.3902	1.1111	1.6629	1.9615	1.9615	1.6629	1.1111	0.3902	1.0000		
9	0.3473	1.0000	1.5321	1.8794	2.0000	1.8794	1.5321	1.0000	0.3473	1.0000	
10	0.3129	0.9080	1.4142	1.7820	1.9754	1.9754	1.7820	1.4142	0.9080	0.3129	1.0000

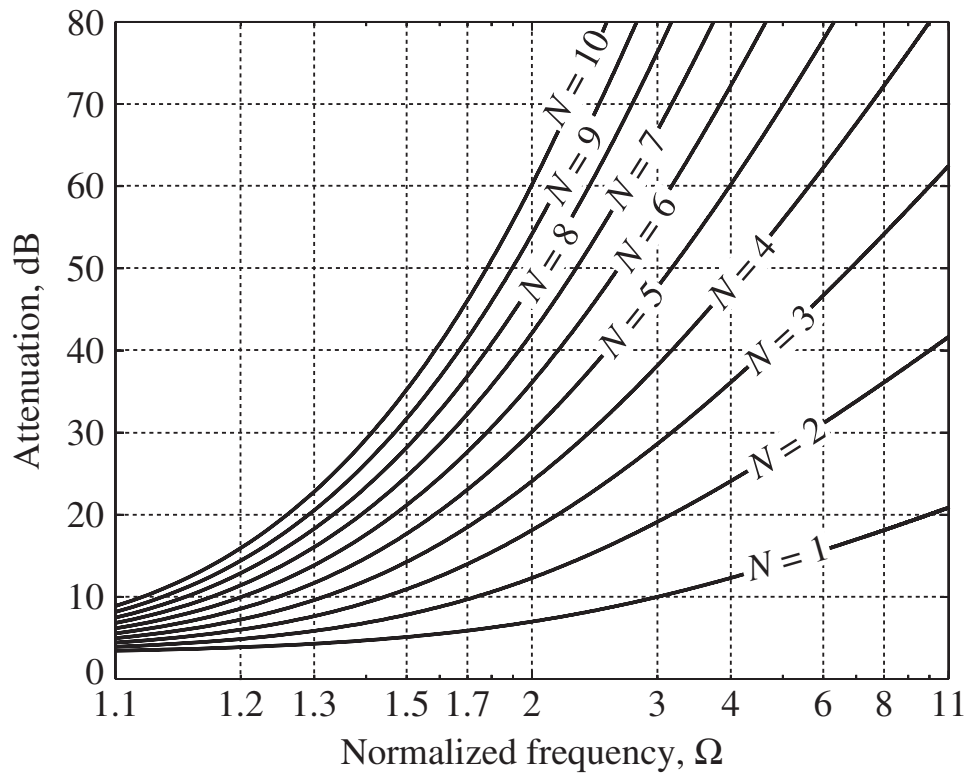


Figure 1-18 Attenuation behavior of maximally flat low-pass filter versus normalized frequency.

Table 1-3 Coefficients for linear phase low-pass filter ($N = 1$ to 10)

N	g_1	g_2	g_3	g_4	g_5	g_6	g_7	g_8	g_9	g_{10}	g_{11}
1	2.0000	1.0000									
2	1.5774	0.4226	1.0000								
3	1.2550	0.5528	0.1922	1.0000							
4	1.0598	0.5116	0.3181	0.1104	1.0000						
5	0.9303	0.4577	0.3312	0.2090	0.0718	1.0000					
6	0.8377	0.4116	0.3158	0.2364	0.1480	0.0505	1.0000				
7	0.7677	0.3744	0.2944	0.2378	0.1778	0.1104	0.0375	1.0000			
8	0.7125	0.3446	0.2735	0.2297	0.1867	0.1387	0.0855	0.0289	1.0000		
9	0.6678	0.3203	0.2547	0.2184	0.1859	0.1506	0.1111	0.0682	0.0230	1.0000	
10	0.6305	0.3002	0.2384	0.2066	0.1808	0.1539	0.1240	0.0911	0.0557	0.0187	1.0000

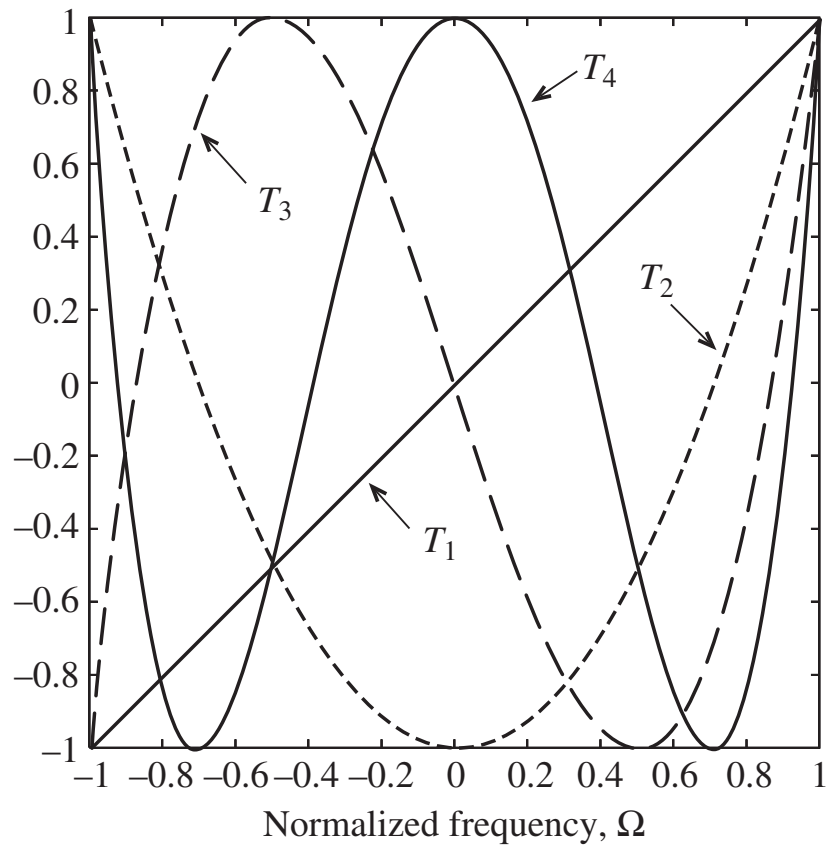


Figure 1-19 Chebyshev polynomials $T_1(\Omega)$ through $T_4(\Omega)$ in the normalized frequency range $-1 \leq \Omega \leq 1$.

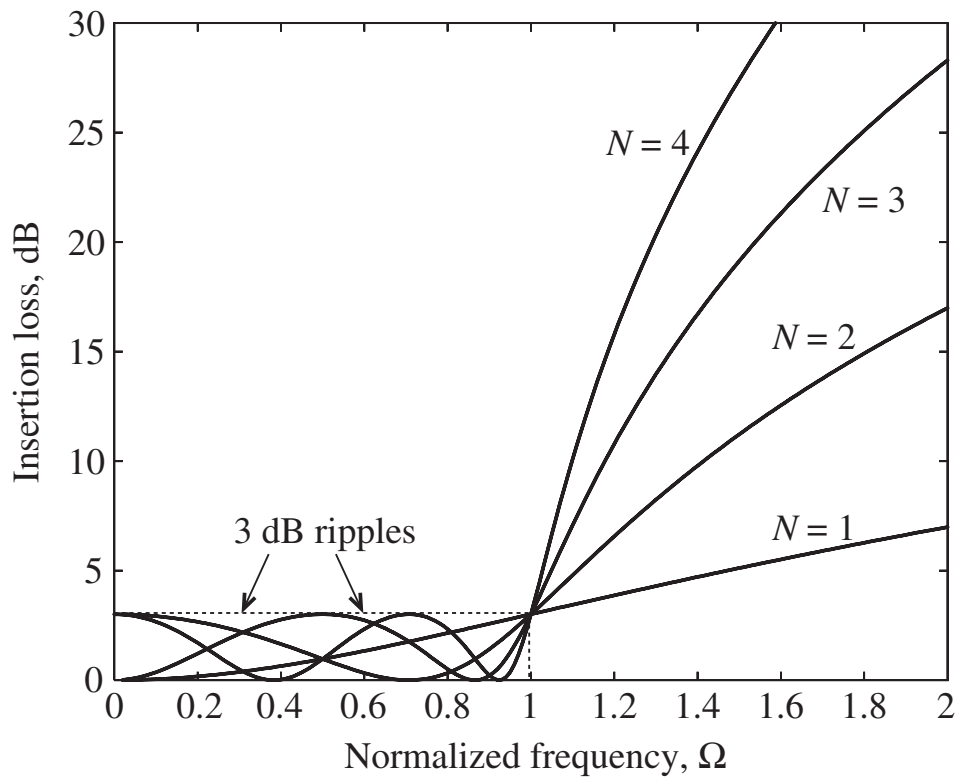
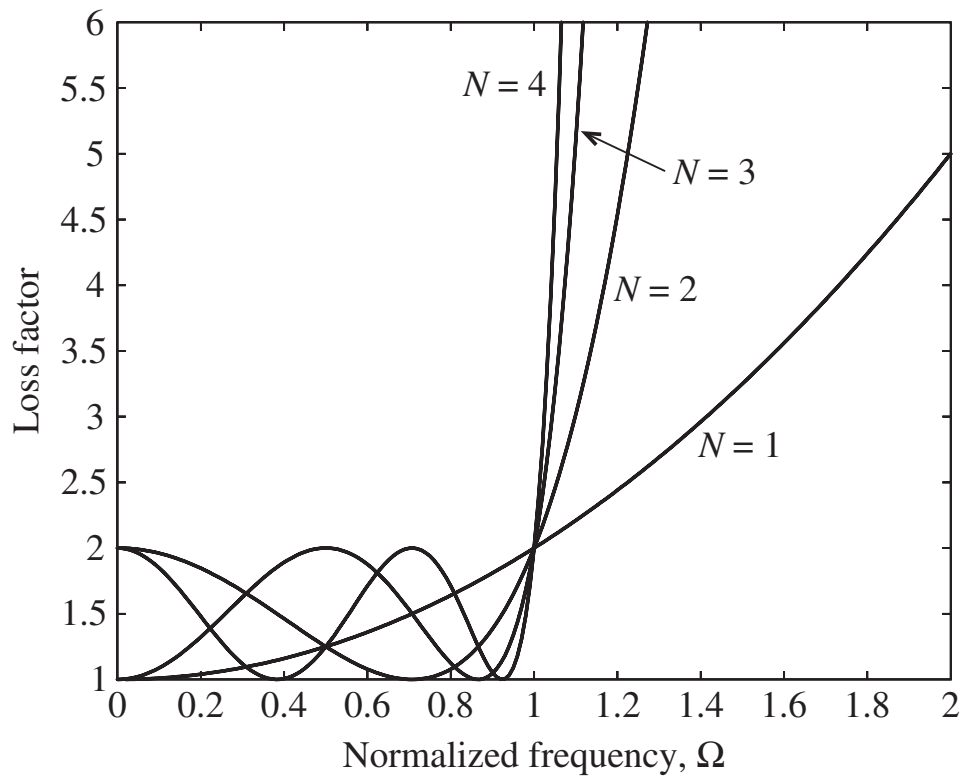


Figure 1-20 Frequency dependence of the loss factor and insertion loss of the Chebyshev low-pass filter.

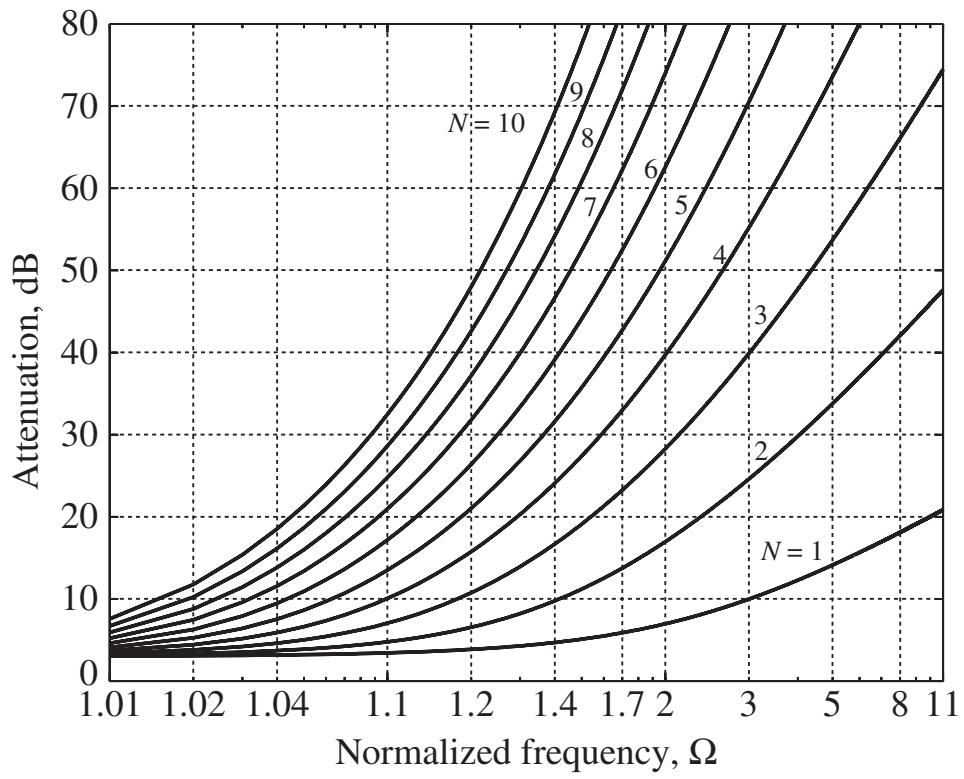


Figure 1-21 Attenuation response for 3 dB Chebyshev design.

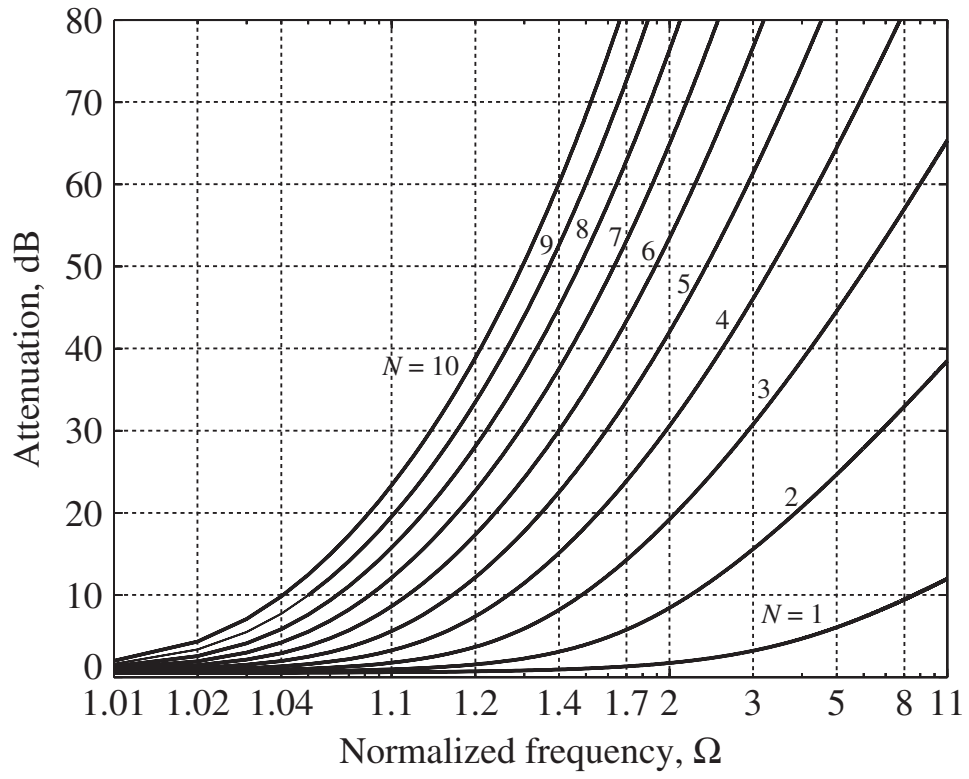


Figure 1-22 Attenuation response for 0.5 dB Chebyshev design.

Table 1-4 (a) Chebyshev filter coefficients; 3 dB filter design ($N = 1$ to 10)

N	g_1	g_2	g_3	g_4	g_5	g_6	g_7	g_8	g_9	g_{10}	g_{11}
1	1.9953	1.0000									
2	3.1013	0.5339	5.8095								
3	3.3487	0.7117	3.3487	1.0000							
4	3.4389	0.7483	4.3471	0.5920	5.8095						
5	3.4817	0.7618	4.5381	0.7618	3.4817	1.0000					
6	3.5045	0.7685	4.6061	0.7929	4.4641	0.6033	5.8095				
7	3.5182	0.7723	4.6386	0.8039	4.6386	0.7723	3.5182	1.0000			
8	3.5277	0.7745	4.6575	0.8089	4.6990	0.8018	4.4990	0.6073	5.8095		
9	3.5340	0.7760	4.6692	0.8118	4.7272	0.8118	4.6692	0.7760	3.5340	1.0000	
10	3.5384	0.7771	4.6768	0.8136	4.7425	0.8164	4.7260	0.8051	4.5142	0.6091	5.8095

Table 1-4 (b) Chebyshev filter coefficients; 0.5 dB filter design ($N = 1$ to 10)

N	g_1	g_2	g_3	g_4	g_5	g_6	g_7	g_8	g_9	g_{10}	g_{11}
1	0.6986	1.0000									
2	1.4029	0.7071	1.9841								
3	1.5963	1.0967	1.5963	1.0000							
4	1.6703	1.1926	2.3661	0.8419	1.9841						
5	1.7058	1.2296	2.5408	1.2296	1.7058	1.0000					
6	1.7254	1.2479	2.6064	1.3137	2.4758	0.8696	1.9841				
7	1.7372	1.2583	2.6381	1.3444	2.6381	1.2583	1.7372	1.0000			
8	1.7451	1.2647	2.6564	1.3590	2.6964	1.3389	2.5093	0.8796	1.9841		
9	1.7504	1.2690	2.6678	1.3673	2.7939	1.3673	2.6678	1.2690	1.7504	1.0000	
10	1.7543	1.2721	2.6754	1.3725	2.7392	1.3806	2.7231	1.3485	2.5239	0.8842	1.9841

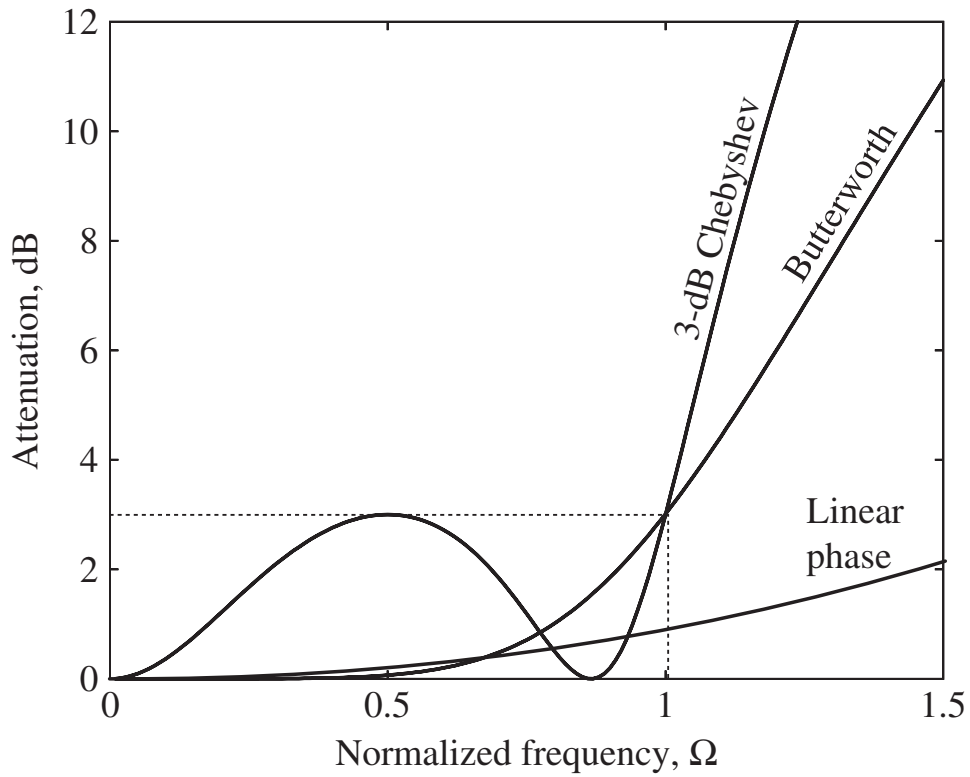


Figure 1-23 Comparison of the frequency response of the Butterworth, linear phase, and 3-dB Chebyshev third-order filters.

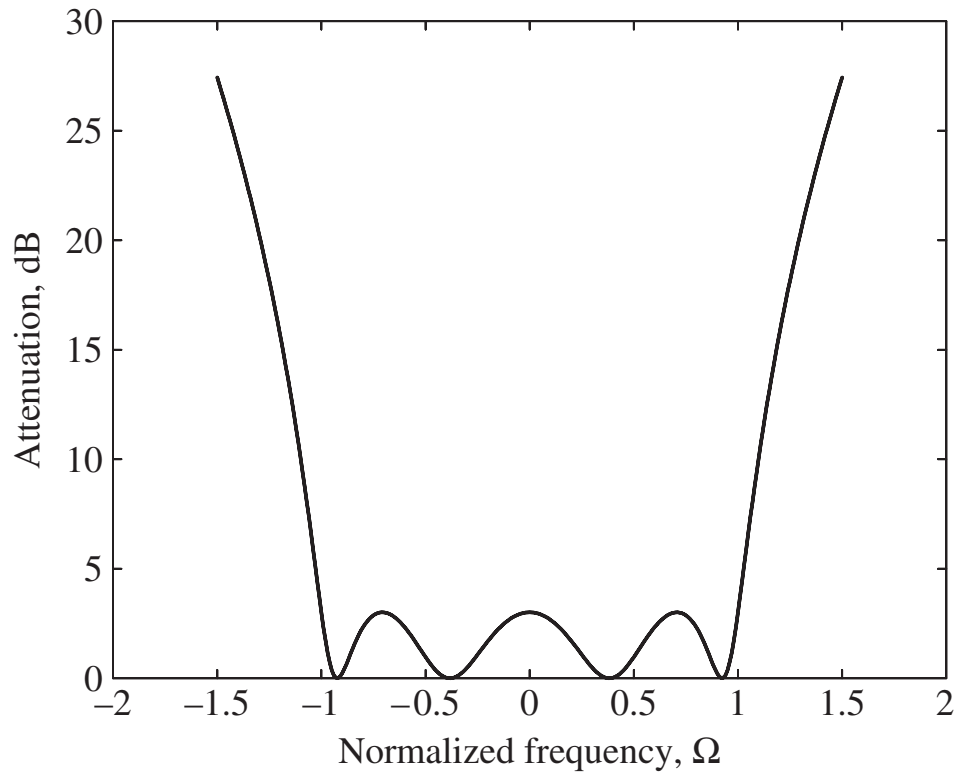


Figure 1-24 Fourth-order low-pass Chebyshev filter with 3 dB ripples in the passband.

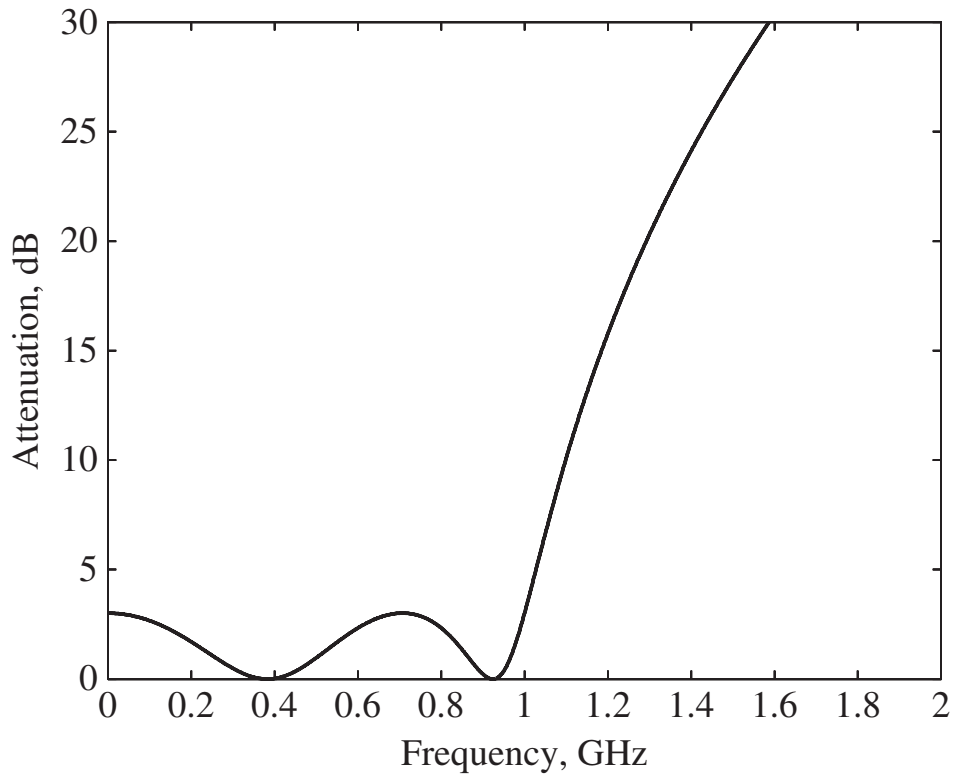


Figure 1-25 Conversion of standard low-pass filter prototype into low-pass realization. Cutoff frequency is $f_c = 1$ GHz.

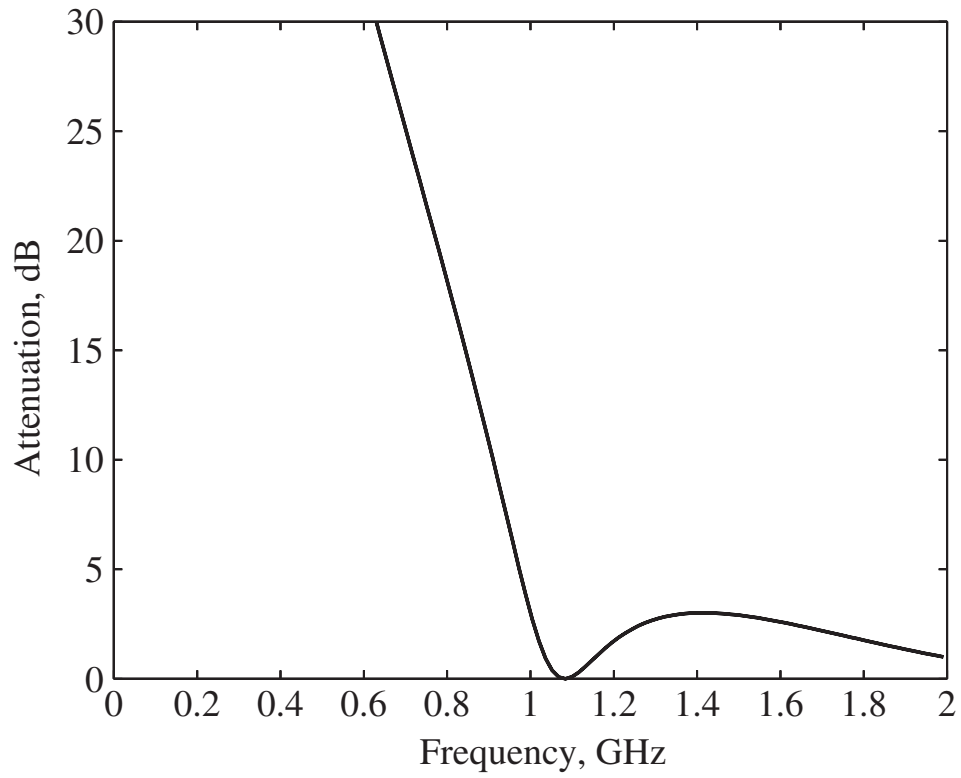


Figure 1-26 Conversion of standard low-pass filter prototype into high-pass realization. Cutoff frequency is $f_c = 1$ GHz.

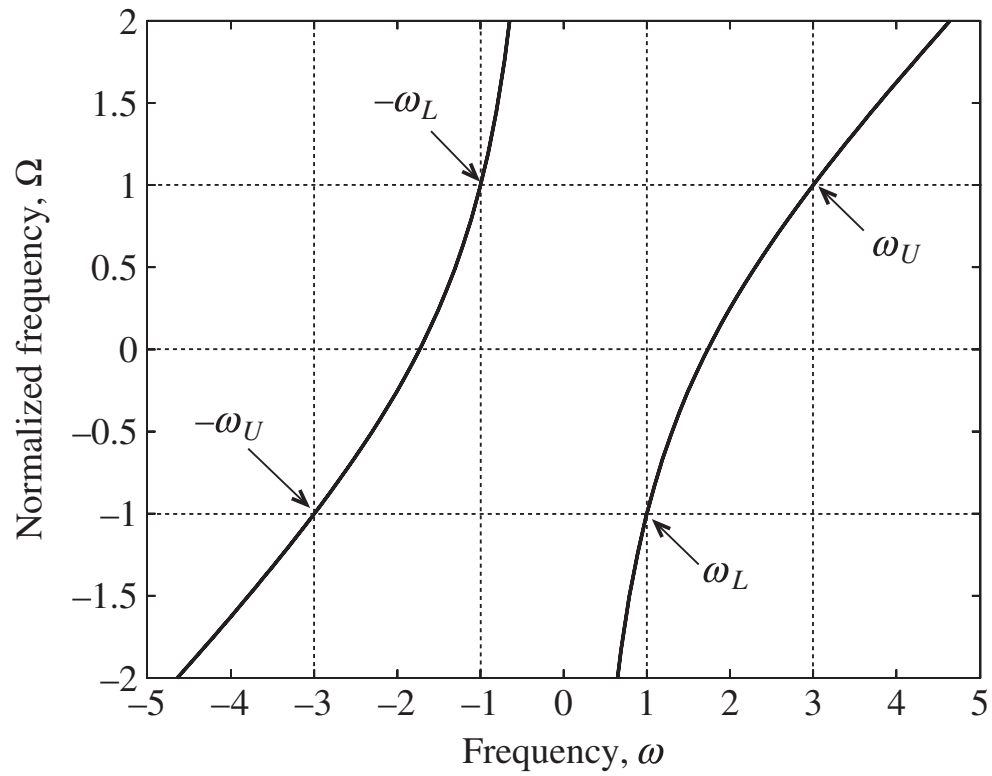


Figure 1-27 Mapping from standard frequency Ω into actual frequency ω . Lower cut-off frequency is $\omega_L = 1$ and upper cutoff frequency is $\omega_U = 3$.

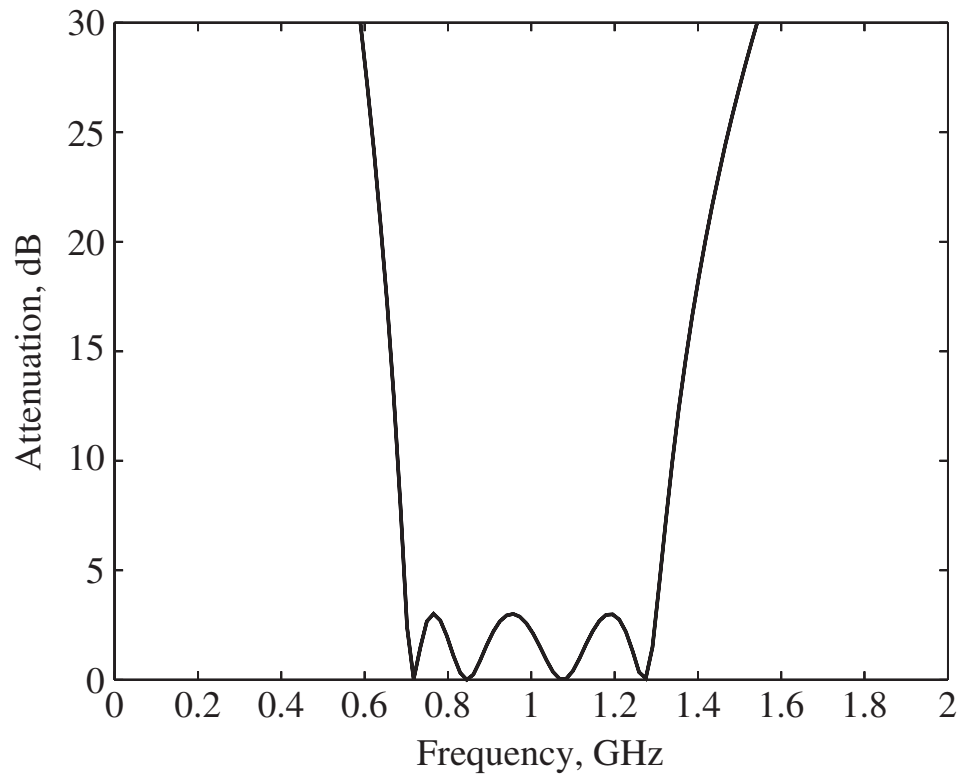


Figure 1-28 Conversion of standard low-pass filter prototype into bandpass realization with lower cutoff frequency $f_L = 0.7$ GHz, upper cutoff frequency $f_U = 1.3$ GHz, and center frequency of $f_0 = 0.95$ GHz.

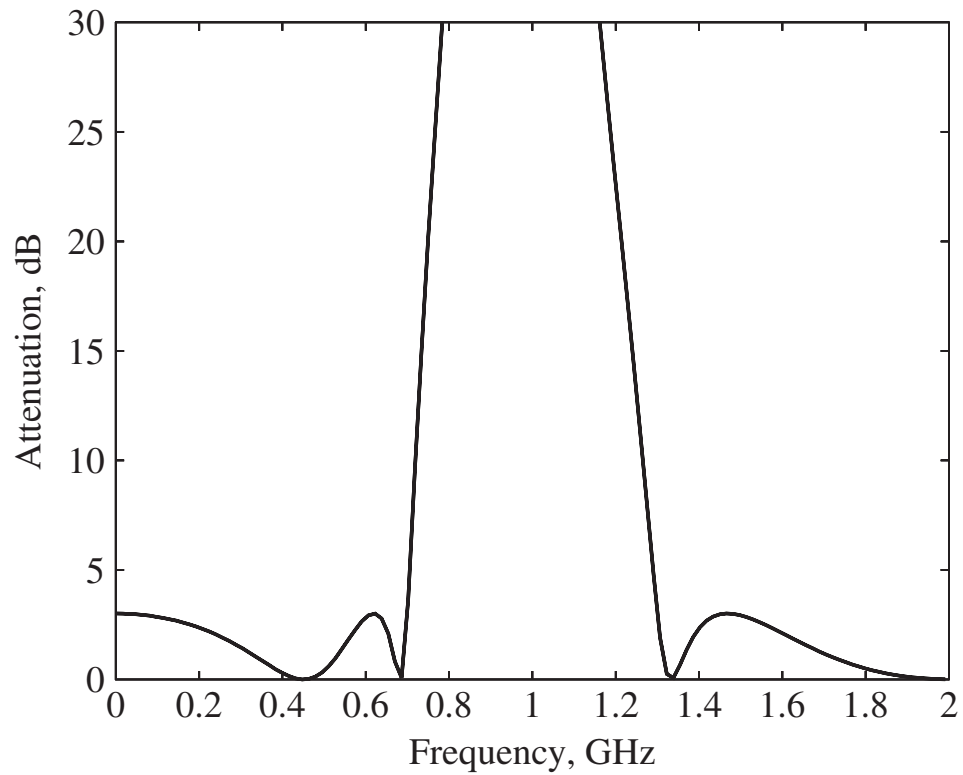



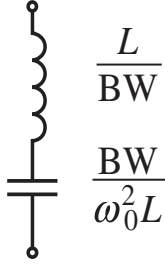
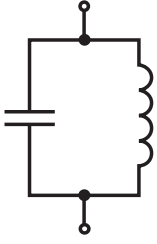



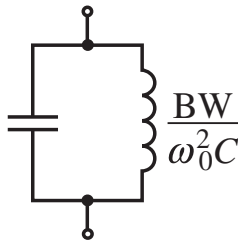



Figure 1-29 Conversion of standard low-pass filter prototype into bandstop realization with center frequency of $f_0 = 0.95$ GHz. Lower cut-off frequency is $f_L = 0.7$ GHz and upper cutoff frequency is $f_U = 1.3$ GHz.

Table 1-5 Transformation between normalized low-pass filter and actual bandpass and bandstop filter $W = \omega_U - \omega_L$, $\omega_0 = \sqrt{\omega_U \omega_L}$

Low-pass prototype	Low-pass	High-pass	Bandpass	Bandstop
 $L = g_k$	 $\frac{L}{\omega_c}$	 $\frac{1}{\omega_c L}$	 $\frac{L}{BW}$ $\frac{BW}{\omega_0^2 L}$	 $\frac{1}{(BW)L}$ $\frac{(BW)L}{\omega_0^2}$
 $C = g_k$	 $\frac{C}{\omega_c}$	 $\frac{1}{\omega_c C}$	 $\frac{C}{BW}$ $\frac{BW}{\omega_0^2 C}$	 $\frac{1}{(BW)C}$ $\frac{(BW)C}{\omega_0^2}$

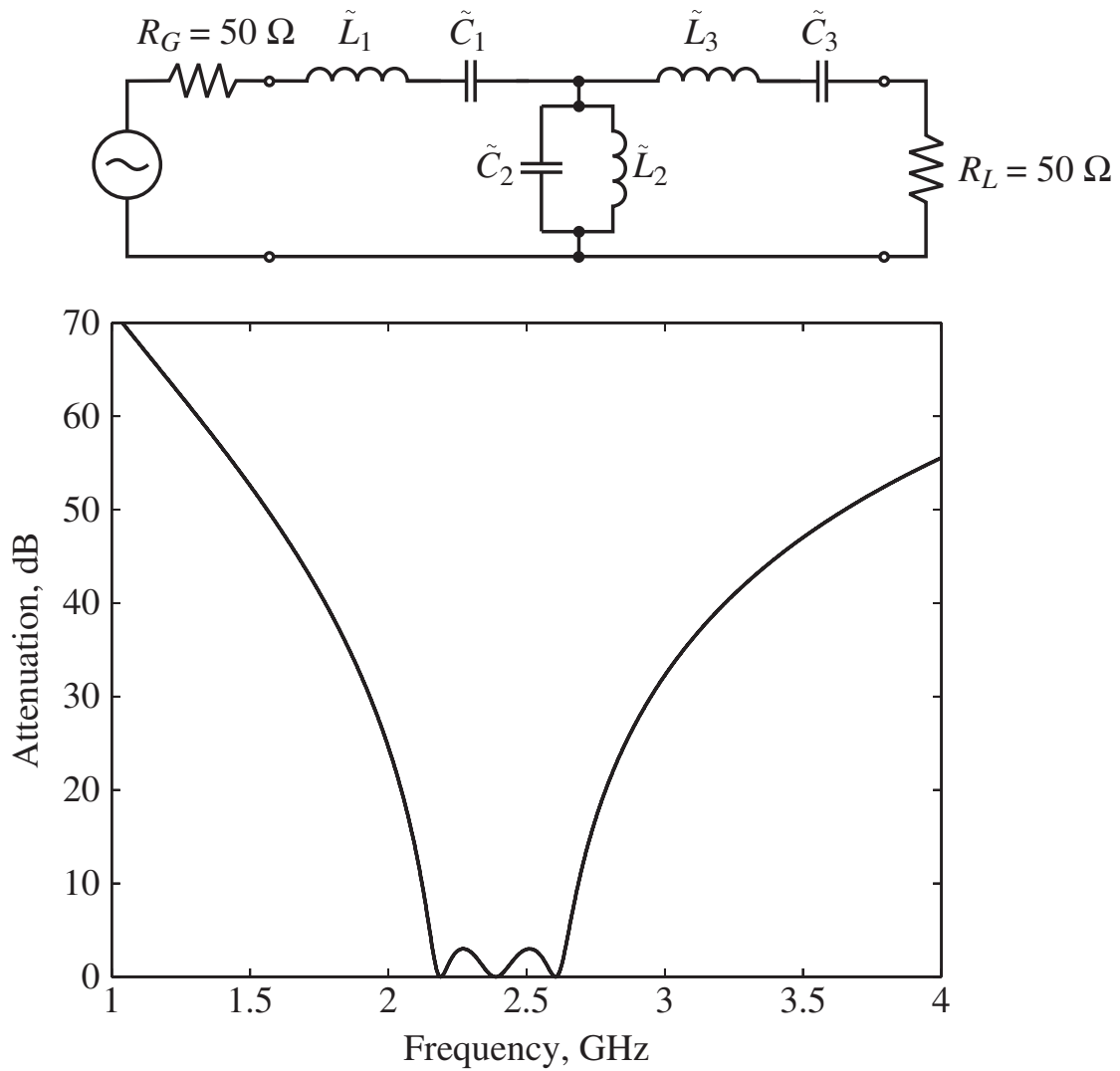
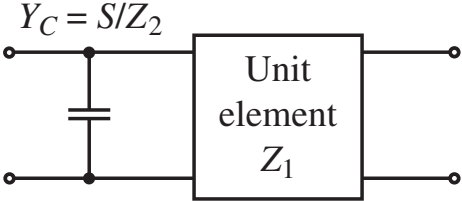
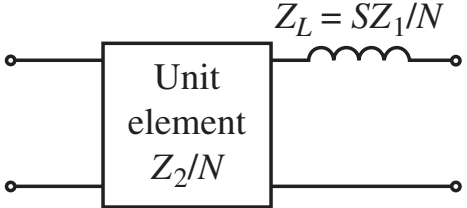
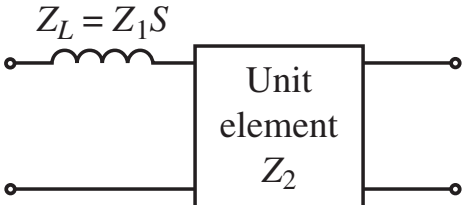
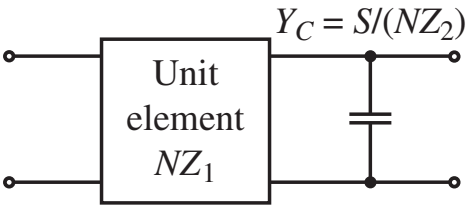
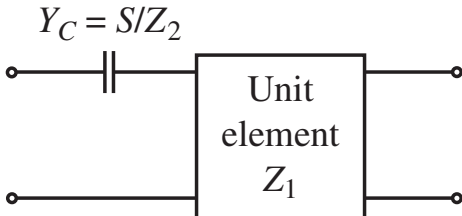
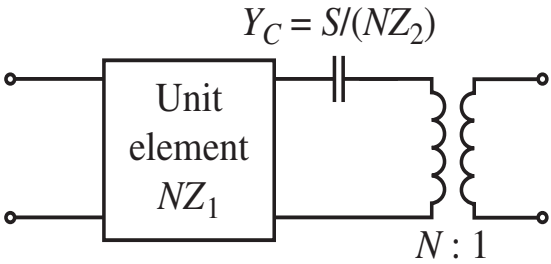
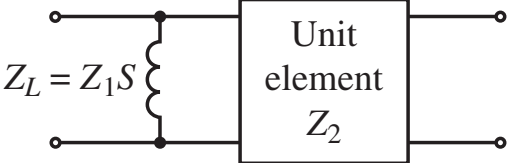
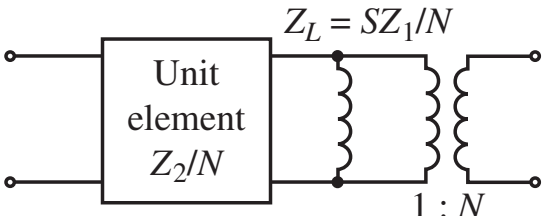


Figure 1-30 Attenuation response of a three-element 3 dB ripple bandpass Chebyshev filter centered at 2.4 GHz. The lower cutoff frequency is $f_L = 2.16$ GHz and the upper cutoff frequency is $f_U = 2.64$ GHz.

Table 1-6 Kuroda's identities

Initial Circuit	Kuroda's Identity
 <p>Initial circuit: A capacitor with admittance $Y_C = S/Z_2$ is connected in parallel to the input of a unit element Z_1.</p>	 <p>Kuroda's Identity: A unit element Z_2/N is connected in series to the input of a unit element Z_1, with an inductor of impedance $Z_L = SZ_1/N$ connected in parallel to the output.</p>
 <p>Initial circuit: An inductor with impedance $Z_L = Z_1 S$ is connected in series to the input of a unit element Z_2.</p>	 <p>Kuroda's Identity: A unit element NZ_1 is connected in series to the input of a unit element Z_2, with a capacitor of admittance $Y_C = S/(NZ_2)$ connected in parallel to the output.</p>
 <p>Initial circuit: A capacitor with admittance $Y_C = S/Z_2$ is connected in series to the input of a unit element Z_1.</p>	 <p>Kuroda's Identity: A unit element NZ_1 is connected in series to the input of a unit element Z_1, with a capacitor of admittance $Y_C = S/(NZ_2)$ connected in parallel to the output, which is also connected to a transformer with turns ratio $N : 1$.</p>
 <p>Initial circuit: An inductor with impedance $Z_L = Z_1 S$ is connected in series to the input of a unit element Z_2.</p>	 <p>Kuroda's Identity: A unit element Z_2/N is connected in series to the input of a unit element Z_2, with an inductor of impedance $Z_L = SZ_1/N$ connected in parallel to the output, which is also connected to a transformer with turns ratio $1 : N$.</p>
$N = 1 + Z_2/Z_1$	

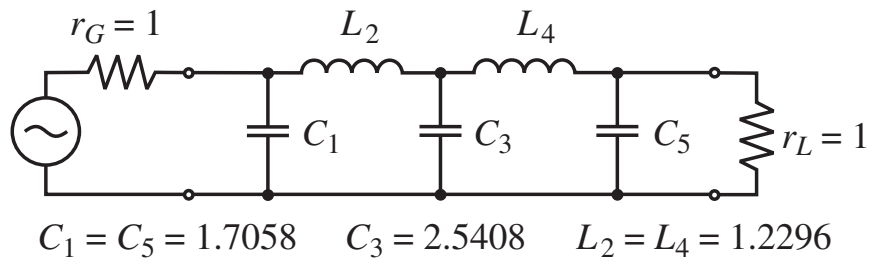


Figure 1-31 Normalized low-pass filter of order $N = 5$.

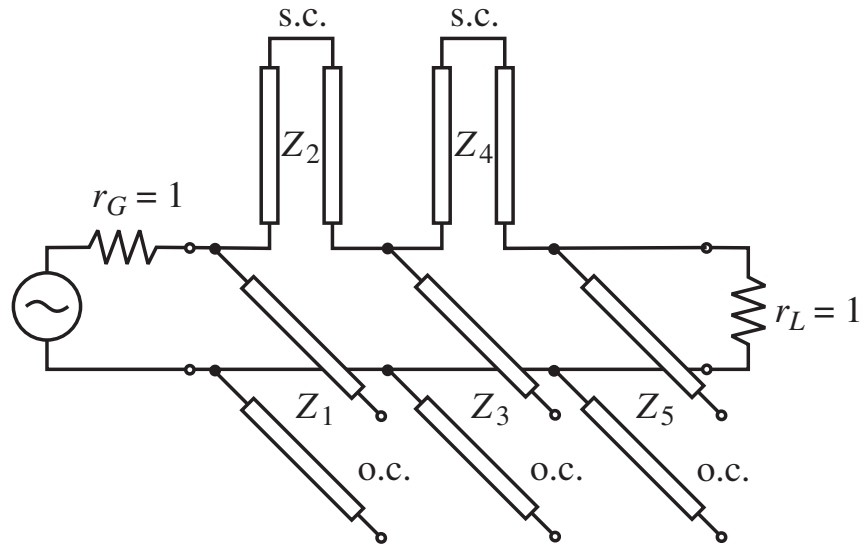


Figure 1-32 Replacing inductors and capacitors by series and shunt stubs (o.c. = open-circuited line, s.c. = short-circuited line).

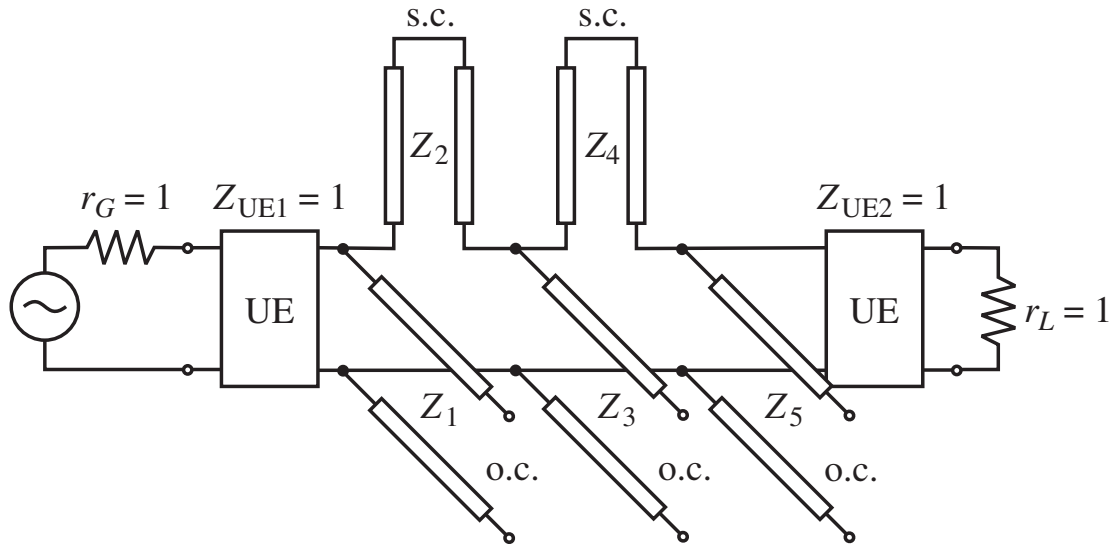


Figure 1-33 Deployment of the first set of unit elements (UE = unit element).

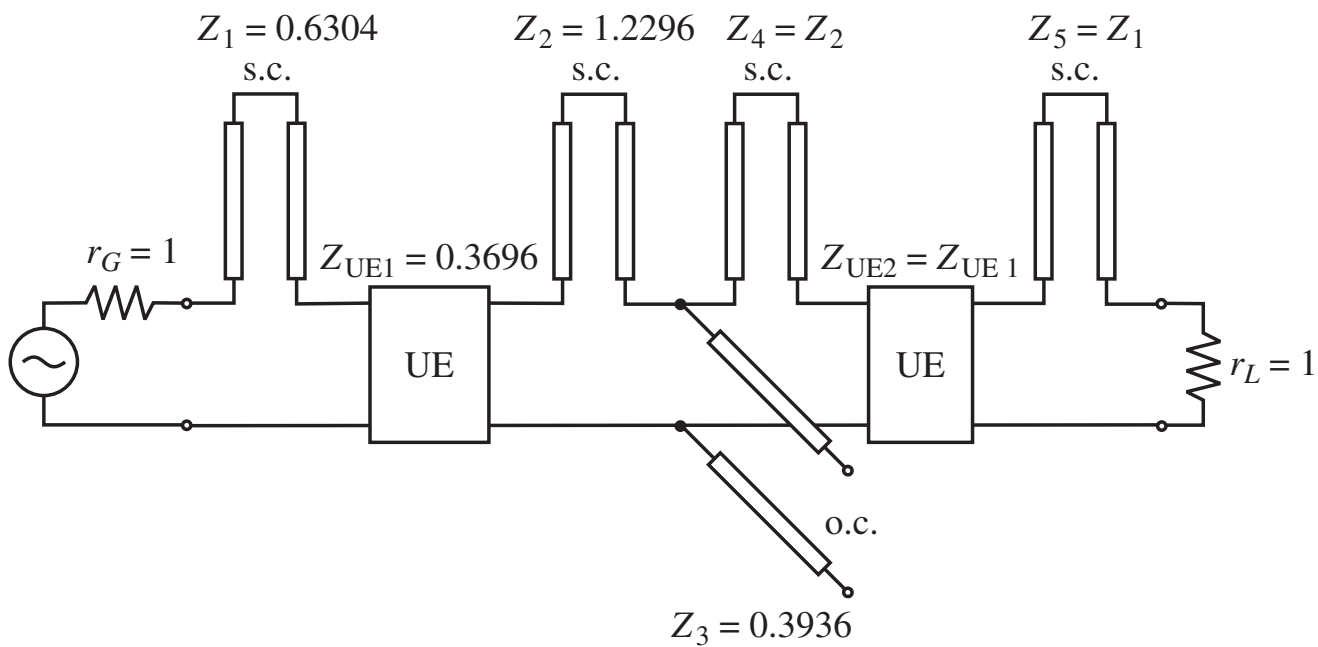


Figure 1-34 Converting shunt stubs to series stubs.

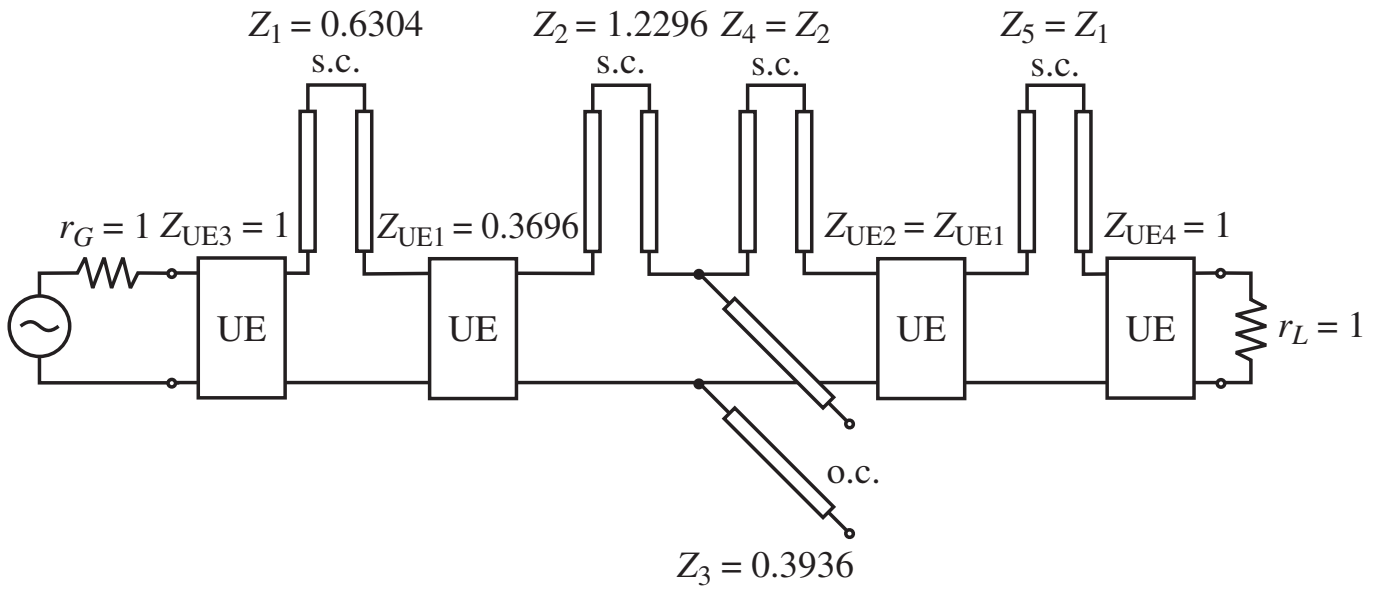


Figure 1-35 Deployment of the second set of unit elements to the fifth-order filter.

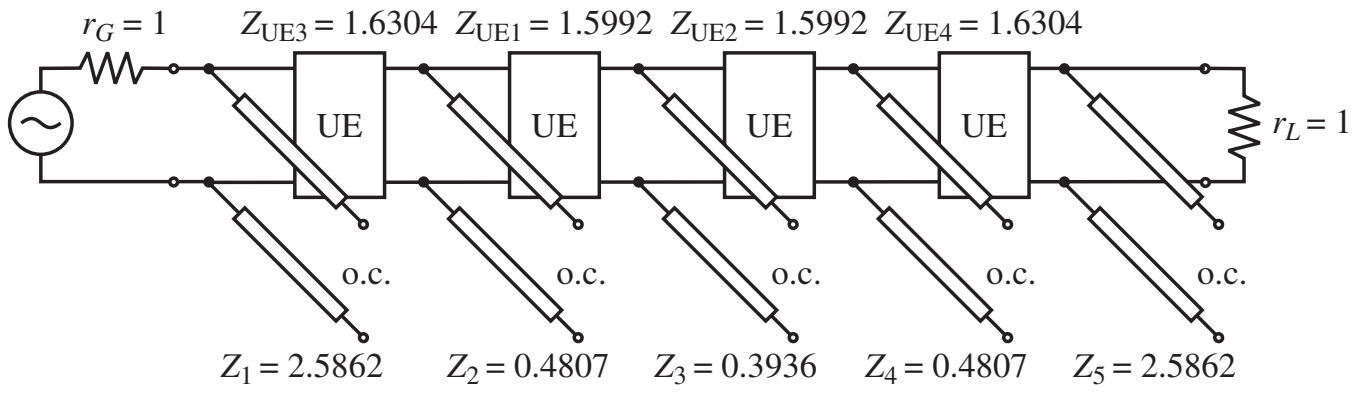
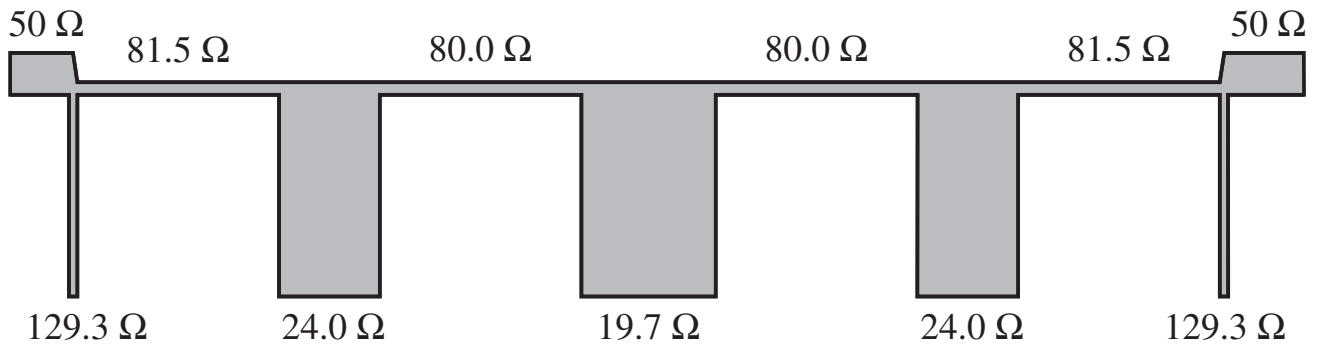
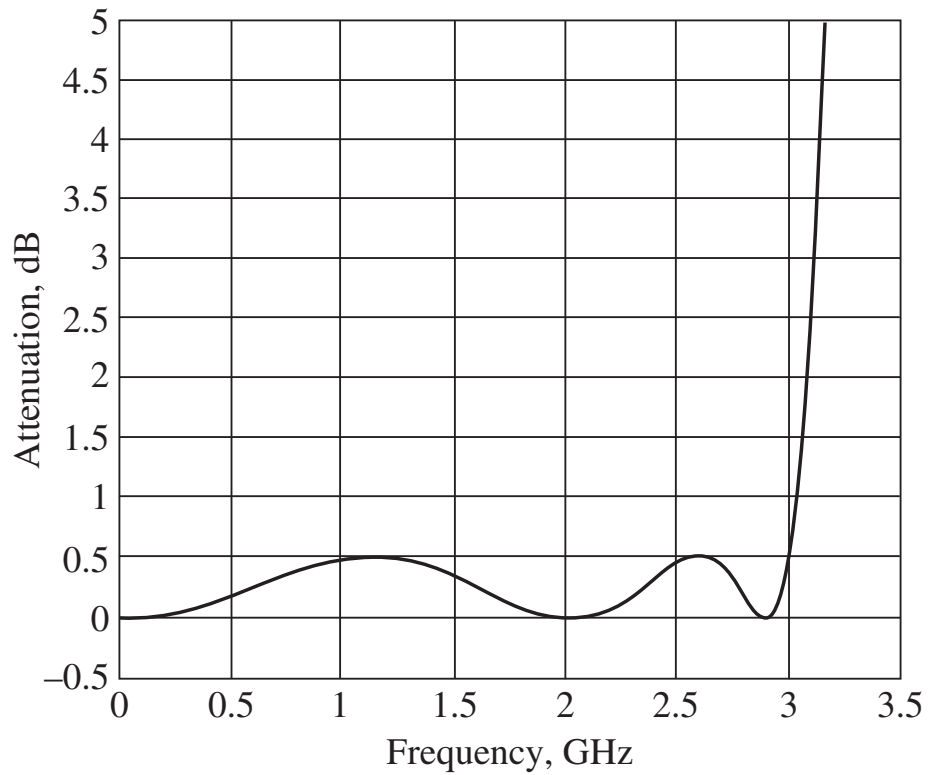


Figure 1-36 Realizable filter circuit obtained by converting series and shunt stubs using Kuroda's identities.



(a) Microstrip line low-pass filter implementation



(b) Attenuation versus frequency response

Figure 1-37 Final microstrip line low-pass filter.

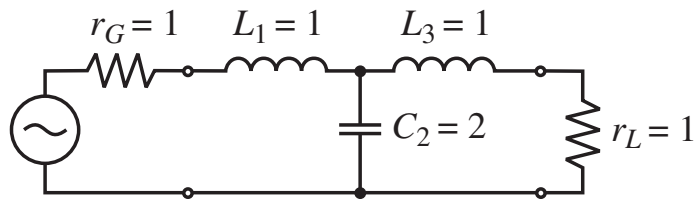


Figure 1-38 Normalized third-order low-pass filter.

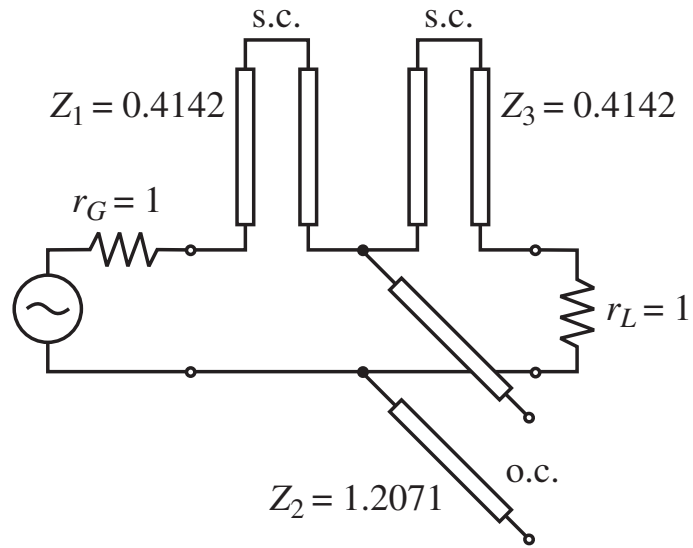
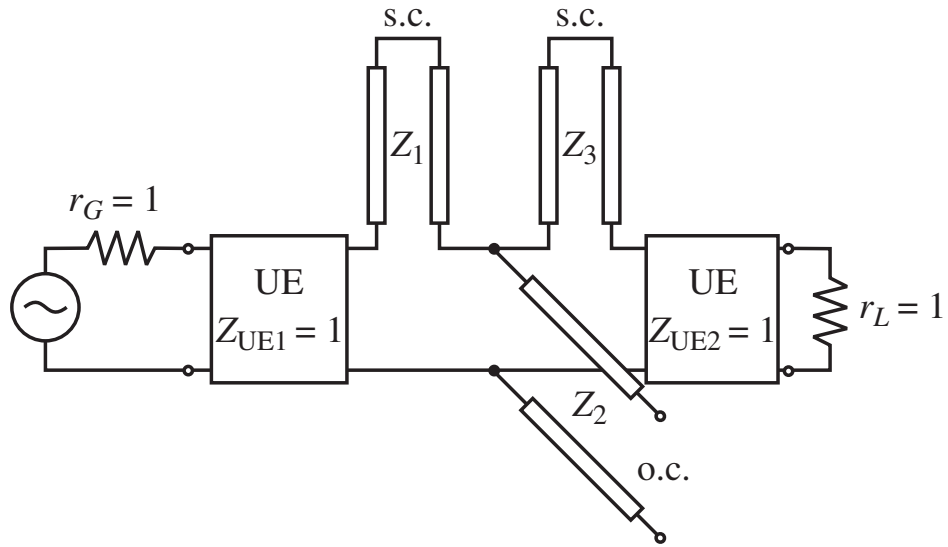
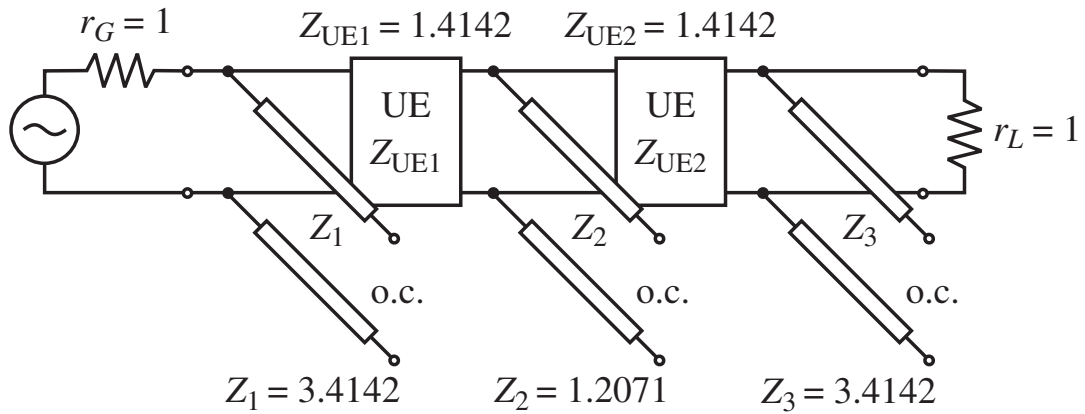


Figure 1-39 Replacing inductors and capacitors by series and shunt stubs.



(a) Unit elements at source and load sides



(b) Conversion from series to shunt stubs

Figure 1-40 Introducing unit elements and converting series stubs to shunt stubs.

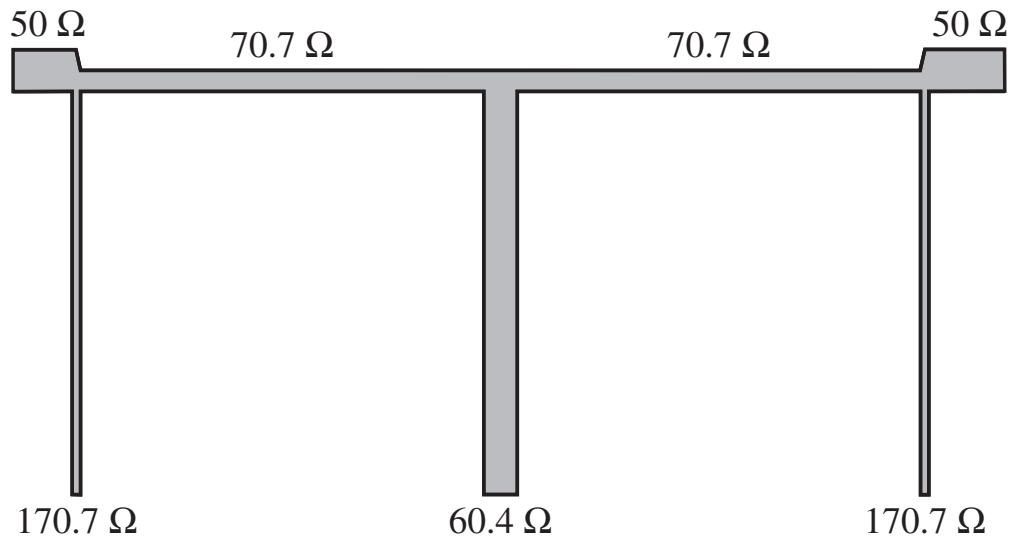


Figure 1-41 Characteristic impedances of final microstrip line implementation of band-stop filter design.

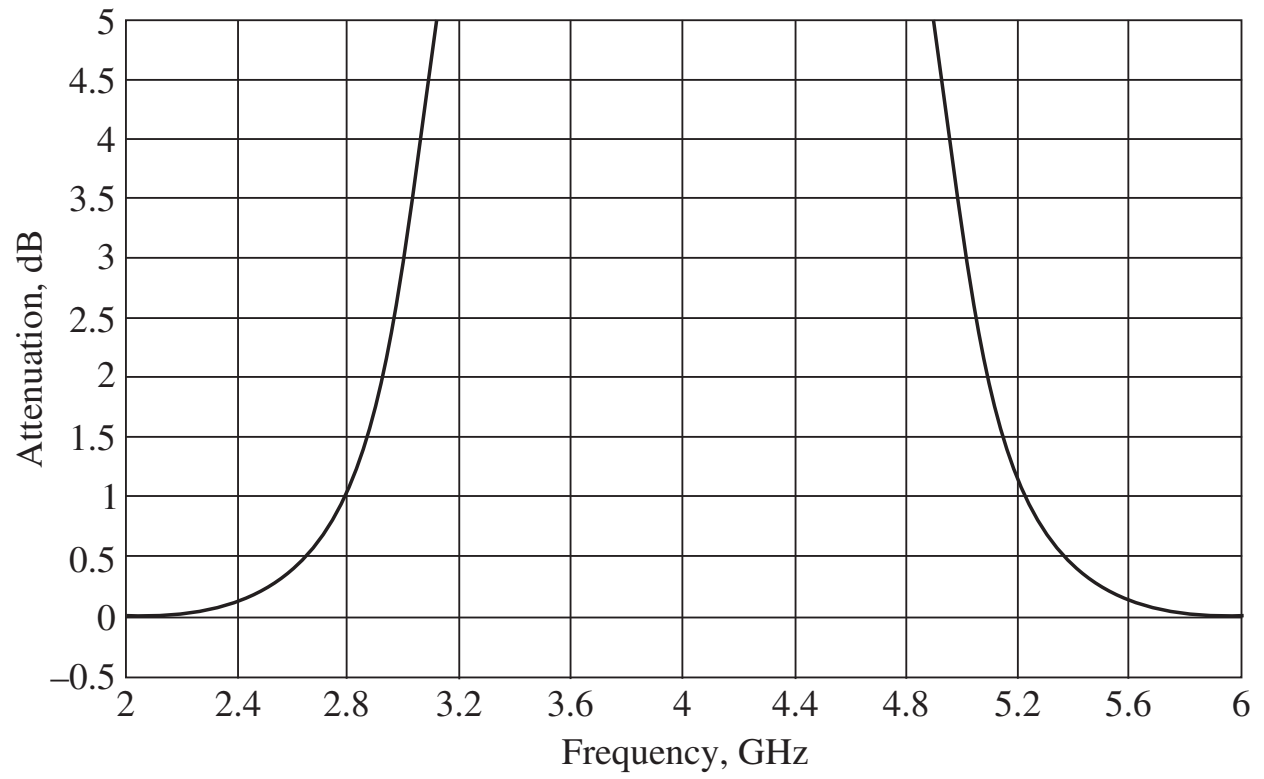


Figure 1-42 Attenuation versus frequency response for third-order bandstop filter.

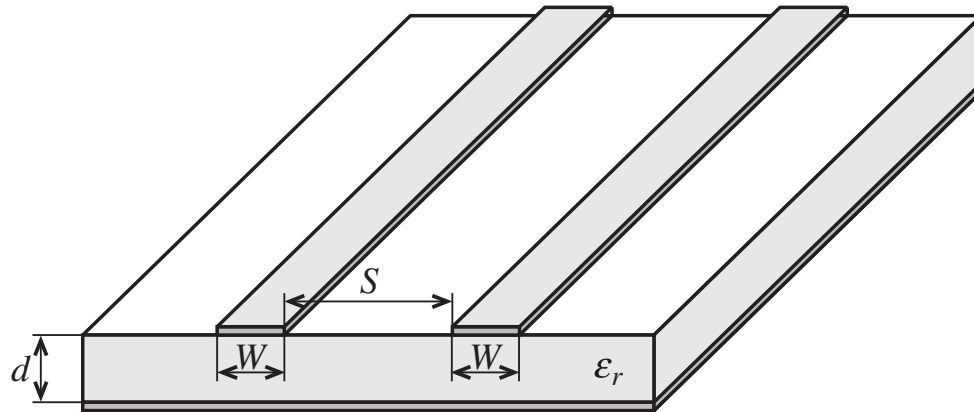


Figure 1-43 Coupled microstrip lines.

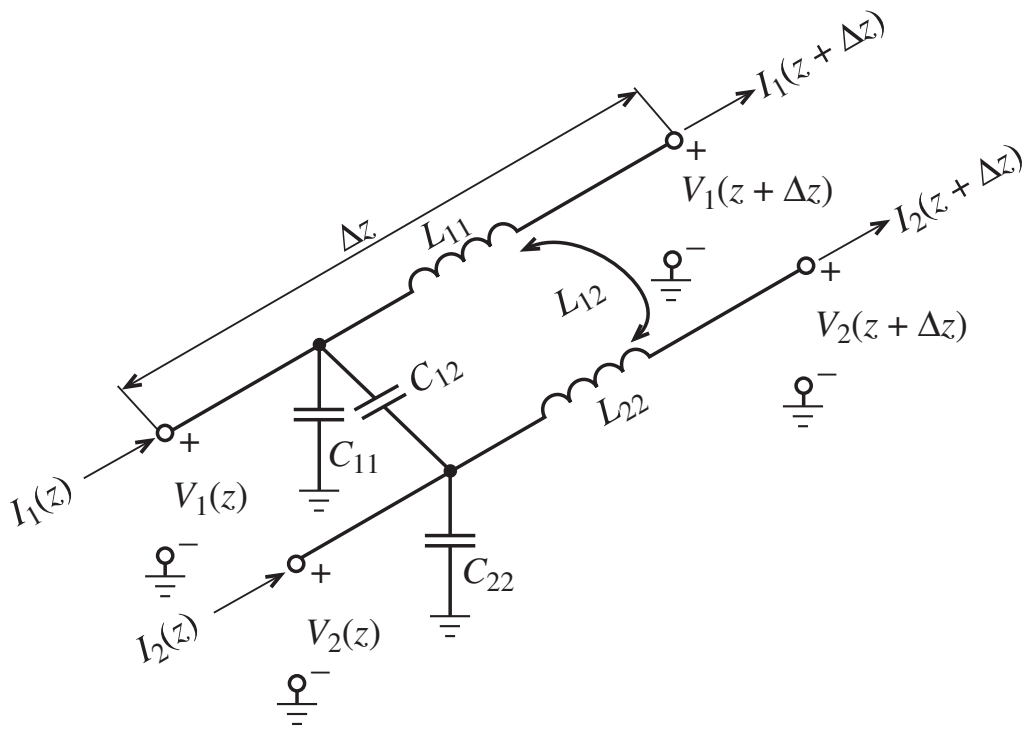


Figure 1-44 Equivalent circuit diagram and appropriate voltage and current definitions for a system of two lossless coupled transmission lines.

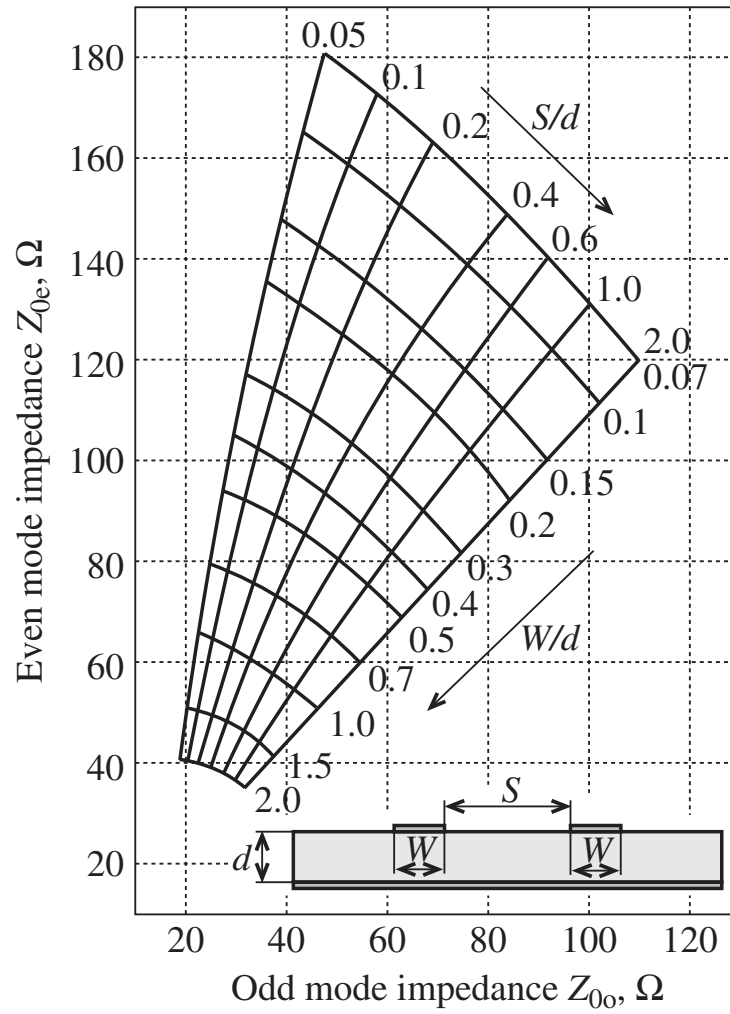


Figure 1-45 Even and odd characteristic impedance for microstrip lines.

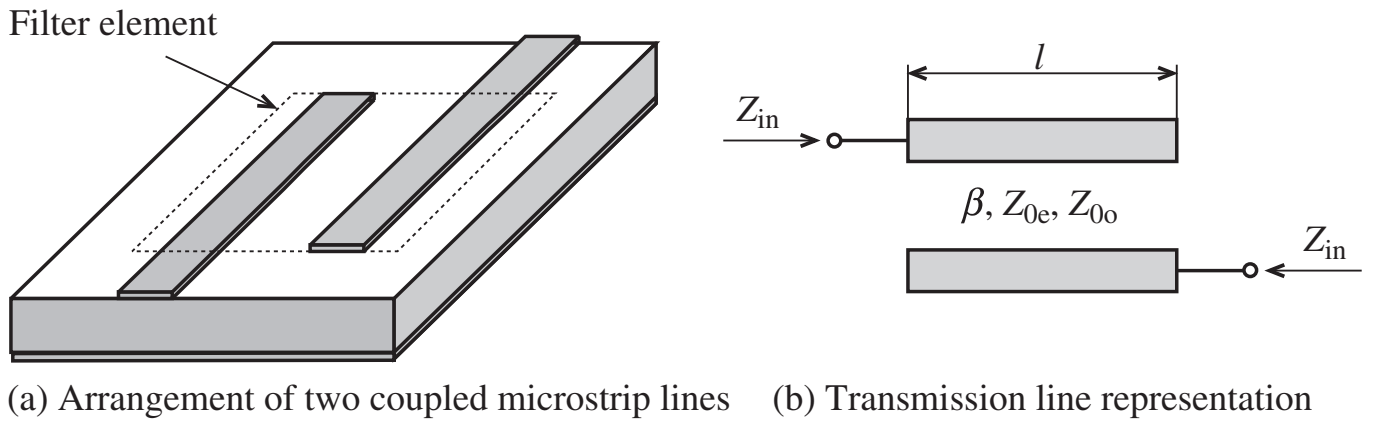


Figure 1-46 Bandpass filter element.

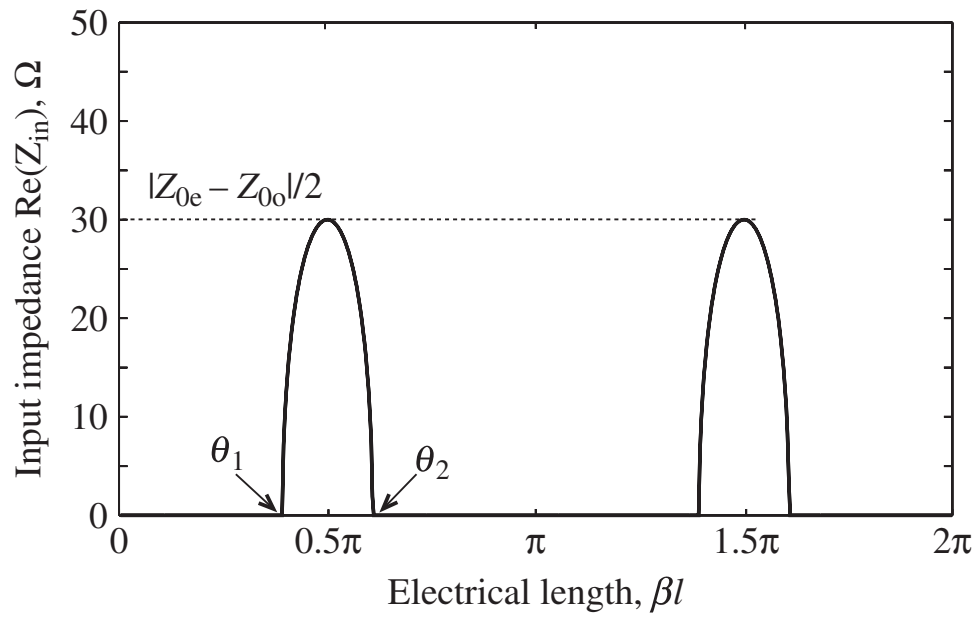


Figure 1-47 Input impedance behavior of equation (5.76). Z_{0e} and Z_{0o} are arbitrarily set to 120Ω and 60Ω , respectively.

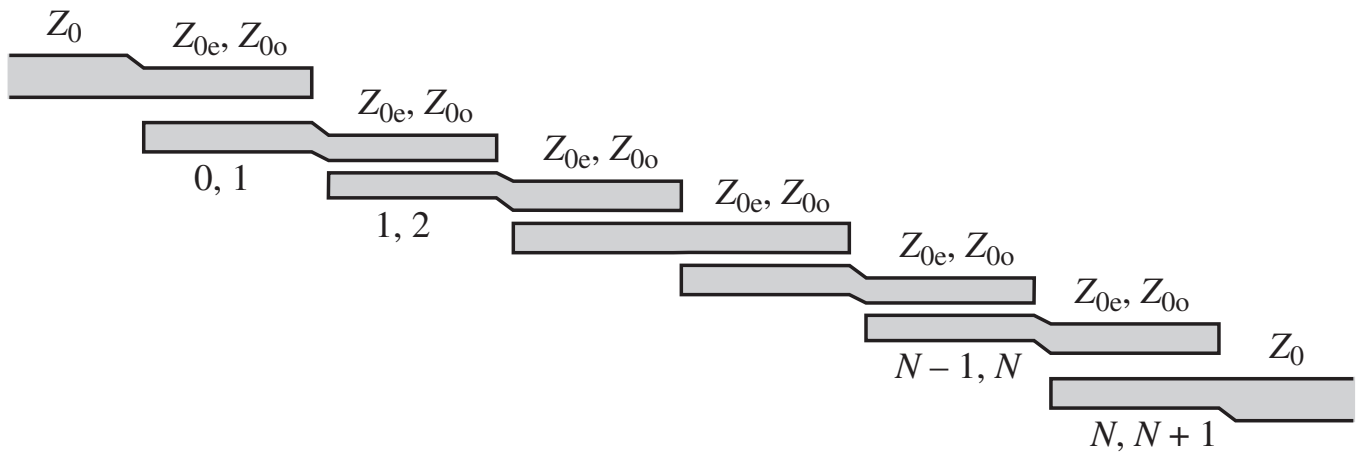


Figure 1-48 Multielement configuration of a fifth-order coupled-line bandpass filter ($N = 5$).

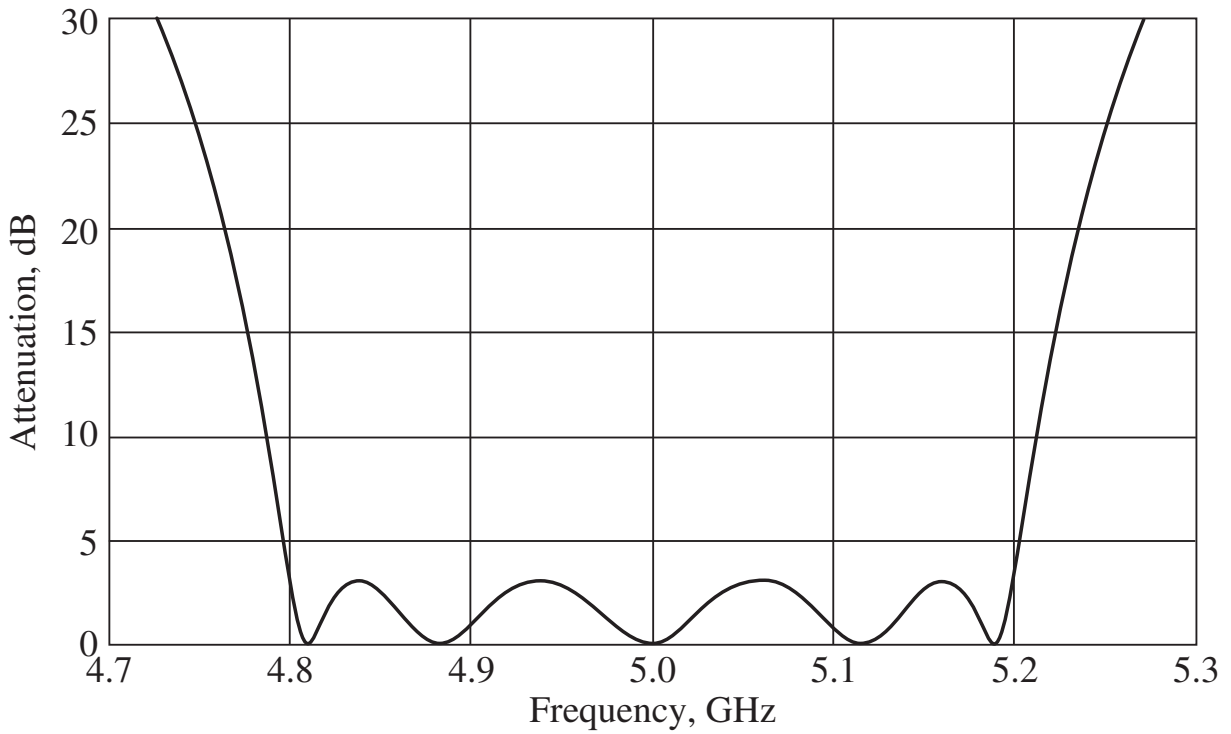
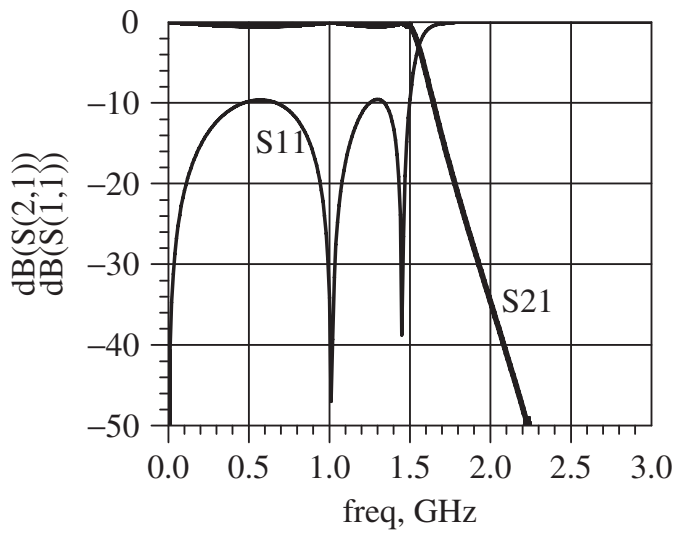
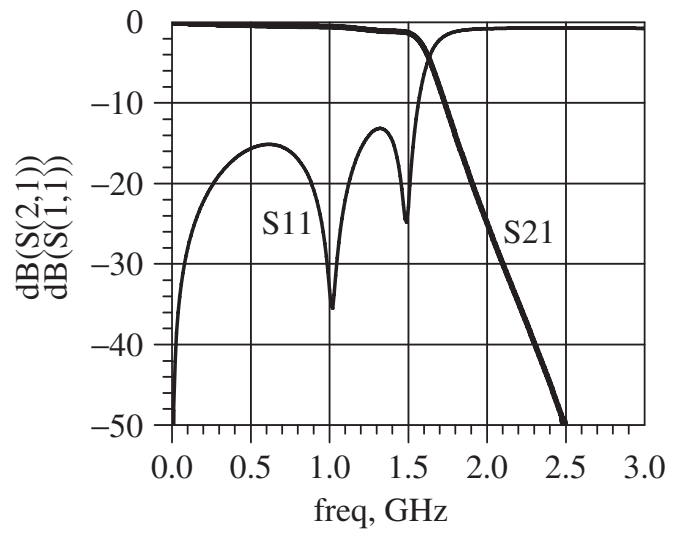


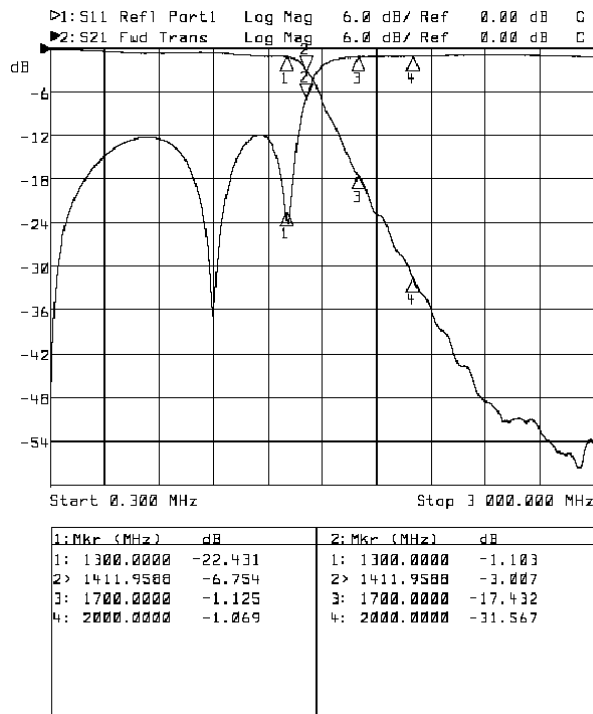
Figure 1-49 Simulations of the fifth-order coupled-line Chebyshev bandpass filter with 3 dB ripple in the passband. The lower cutoff frequency is 4.8 GHz and the upper cutoff frequency is 5.2 GHz.



(a)



(b)

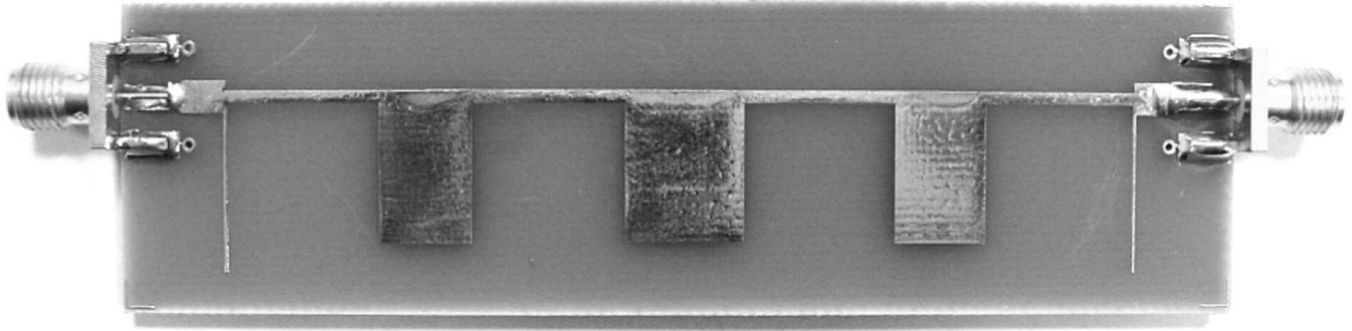


(c)

Figure 1-50 S-parameters of the 1.5 GHz microstrip low-pass filter: (a) Matlab simulation, (b) ADS simulation, (c) network analyzer measurement.



(a)



(b)

Figure 1-51 Microstrip pattern for the 1.5 GHz low-pass filter: (a) ADS simulation, (b) PCB implementation.